UNIVERSITÀ
DEGLI STUDI
DI PADOVA

Head Office: Università degli Studi di Padova

Department of Biology

Ph.D. COURSE IN BIOSCIENCES
CURRICULUM BIOCHEMISTRY AND BIOTECNOLOGY
SERIES XXX

THE MITOCHONDRIAL PROTEIN WHIRLY2 REGULATES SEED GERMINATION AND EARLY STAGES OF GROWTH IN *ARABIDOPSIS THALIANA*

Thesis written with the financial contribution of Fondazione Cariparo

Coordinator: Prof. Ildikò Szabò
Supervisor: Prof. Michela Zottini

Ph.D. Student: Serena Golin

SUMMARY

ABSTRACT

Variations in amount and structural integrity of organellar DNA are tightly regulated by nuclear-organelle cross-talk. Whirly proteins are DNA binding proteins that were shown to play a role in organellar DNA maintenance and organization [Marechal et al. 2008; Cappadocia et al 2010]. *Arabidopsis thaliana* has three Whirly proteins with different subcellular localization: Whirly1 and Whirly3 are targeted to chloroplasts, while Whirly2 is targeted to mitochondria [Krause et al. 2005]. *WHIRLY2* gene expression is related to early plant development, being expressed in imbibed seeds, shoot apex and roots of young seedlings. A T-DNA insertional mutant for the *WHIRLY2* gene shows an obvious phenotype on seeds, germination and early stages of plant growth. At subcellular level Whirly2 regulates mitochondria morphology, dynamics and functionality of the electron transport chain. Transmitted electron microscopy (TEM) revealed that Whirly2 is a major mitochondrial nucleoids organizer, and it influences both mtDNA and ptDNA copy number. Moreover, our results suggest a coordination of *WHIRLY* genes that controls expression of target genes of organellar signals upon development and stress conditions.

INTRODUCTION

Plant cells comprise three organelles (nucleus, plastids and mitochondria) that possess and maintain genetic information. Among these three organelles, the nucleus carries the largest part of genomic information on chromosomes [Maréchal *et al*, 2008]. Organelles have retained a genome, but present-day organelle genomes are severely reduced and encode few proteins. In fact, mitochondria and plastids are composed of 1500 and 3000 proteins, respectively, with >95% of these proteins encoded by nuclear-located genes [Woodson and Chory, 2008]. The compartmentalization of genomes requires a coordination of the gene expression among different subcellular compartments to guarantee the correct concentration of organelle proteins and to maintain organelle function [Pfannschmidt, 2010]. It has been shown that two-way communication pathways exist between the nucleus and mitochondria and chloroplasts, called anterograde (nucleus to organelle) and retrograde (organelle to nucleus) signalling pathways (**Figure 1**) [Ng *et al,* 2013]. In plant cells, chloroplast and mitochondria have complex metabolic interdependencies. For instance, photosynthesis can use mitochondrial products and it provides compounds for mitochondrial respiration (O_2 and malate). Mitochondria dissipate redox equivalents from the chloroplast, which protects the chloroplast from photoinhibition. The chloroplast provides haem precursors to the mitochondria and metabolic compounds [Woodson and Chory, 2008]. However, there is no evidence of direct signalling between chloroplasts and mitochondria, although molecules such as active oxygen species and ascorbate, and mitochondrially produced nitric oxide, have been suggested as candidate signalling molecules [Raghavendra and Padmasree, 2003].

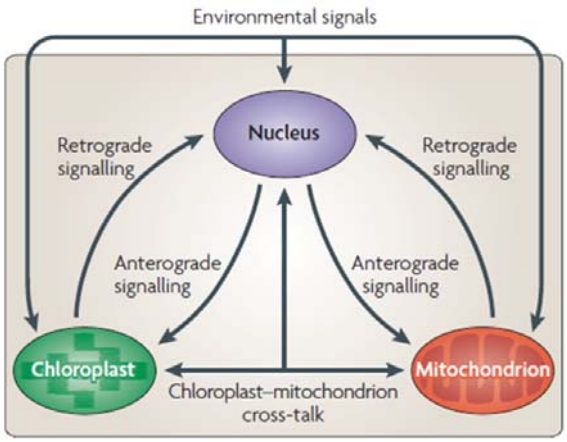

Figure 1: *An overview of genome coordination between the nucleus and intracellular organelles. The diagram depicts communication between the nucleus, chloroplast and mitochondrion [Figure adapted from Woodson and Chory, 2008].*

Retrograde signalling in plants

Anterograde mechanisms coordinate gene expression in organelles in response to endogenous and environmental stimuli that are perceived by the nucleus [Woodson and Chory, 2008]. Conversely, nuclear gene expression is also influenced by signals that originate from within the organelles, mitochondria, or chloroplasts and is referred to as retrograde regulation [Ng *et al,* 2013]. Retrograde mechanisms have evolved to communicate the functional and developmental state of organelles to the nucleus, which can then modulate anterograde control and cellular metabolism accordingly. Since then, diverse types of retrograde signalling pathways, depending on the trigger sources and signals, have been reported. The classical, or linear, model of retrograde signalling describes that specific signals produced in the organelles by different developmental and environmental cues can move into the nucleus where they elicit specific gene regulation [Estavillo *et al*, 2013]. Two principal modes of transfer of retrograde signalling molecules present themselves: transfer by passive diffusion or active transport involving specific transporters (**Figure 2 A and B**) [Leister, 2012]. In an extreme case, the signalling molecules could be delivered directly to its target if organelle and nucleus were physically connected (**Figure 2 C**). In fact, stromules might represent such connection points between plastids and the nucleus [Leister, 2012]. Stromules are stroma-filled tubules that extend from the surface of plastids, are extremely variable in length and are highly dynamic structures. Interestingly, stromules are induced by stress treatments, including drought and salt stress, and application of ABA, conditions which are also thought to be associated with retrograde signalling [Gray *et al*, 2012; Leister, 2012].

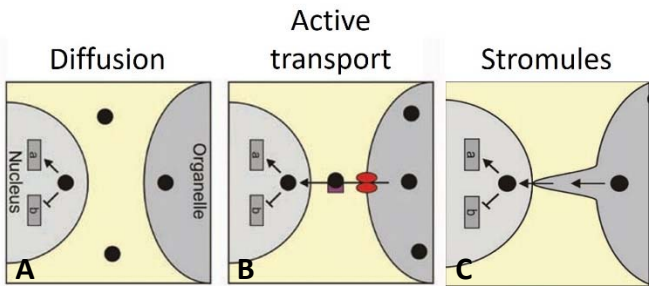

Figure 2: *Schematic overview of the mode of operation for retrograde signalling.* ***(A)*** *Diffusion;* ***(B)*** *Active transport;* ***(C)*** *Direct delivery of the signalling molecule to the nucleus via stromules [Figure adapted from Leister 2012].*

Several retrograde signals are employed for genome coordination, instructing adaptive responses to environmental and developmental conditions or to inform the nucleus of cellular stress. Even if different retrograde candidate signalling pathways and molecules have been identified during the last three decades, the inter-organellar crosstalk remained unfocused and unclear. The significance of a highly orchestrated and interlinked metabolic balance between growth and adaptation to environmental cues positions the cellular metabolic hubs involved in metabolism and energy production, the chloroplast and mitochondria, as the operational control centres of retrograde signalling [de Souza et al, 2017].

Chloroplast retrograde signaling

The chloroplast, as the cell's metabolic hub, is the site of photosynthesis; de novo biosynthesis of fatty acids; production of fatty-acid-derived metabolites, such as amino acids and starches; and hormone metabolisms. To safeguard these central processes against frequent and prevailing challenges, the chloroplast thus functions not only as a central metabolic hub but also as an environmental sensor that perceives stress and produces retrograde signals to coordinale nuclear-encoded adaptive responses [de Souza et al 2017]. The best-characterized chloroplast retrograde signalling pathway involves tetrapyrrole intermediates of the chlorophyll biosynthetic pathway (**Figure 3 A**). Higher plants use Mg–protoIX as a chloroplast signalling molecule. In *Arabidopsis thaliana*, undeveloped chloroplasts that have suffered photooxidative damage, owing to the lack of protective carotenoids, accumulate Mg–protoIX, which leads to the repression of nuclear genes that encode photosynthesis related proteins [Woodson and Chory, 2008]. Mutants that block this retrograde signalling have been isolated (*genomes uncoupled* or *gun* mutants). *Gun* mutants sustained expression of photosynthesis-related genes, including *LIGHT-HARVESTING COMPLEX B (LHCB,* coding for chlorophyll *a/b*-binding protein*)*, under photobleaching stress [de Souza et al, 2017; Susek et al, 1993]. Moreover, Sun et al 2011, reported that one or more retrograde signals

activate proteolytic cleavage and nuclear localization of a chloroplast envelope–bound transcription factor designated PLANTHOMEODOMAIN–TYPETRANSCRIPTION FACTOR WITH TRANSMEMBRANE DOMAINS (PTM) and that the accumulation of PTM in the nucleus activates (*ABSCISIC ACID INSENSITIVE*) *ABI4* transcription (**Figure 3 B**). Other plastidial metabolites implicated in retrograde communications include 3'-phosphoadenosine 5'-phosphate (PAP), β-cyclocitral (β-cyc), 2-*C*-methyl-D-erythritol 2,4-cyclodiphosphate (MEcPP), ROS, fatty acids (FAs), and their corresponding derivatives [de Souza et al, 2017].

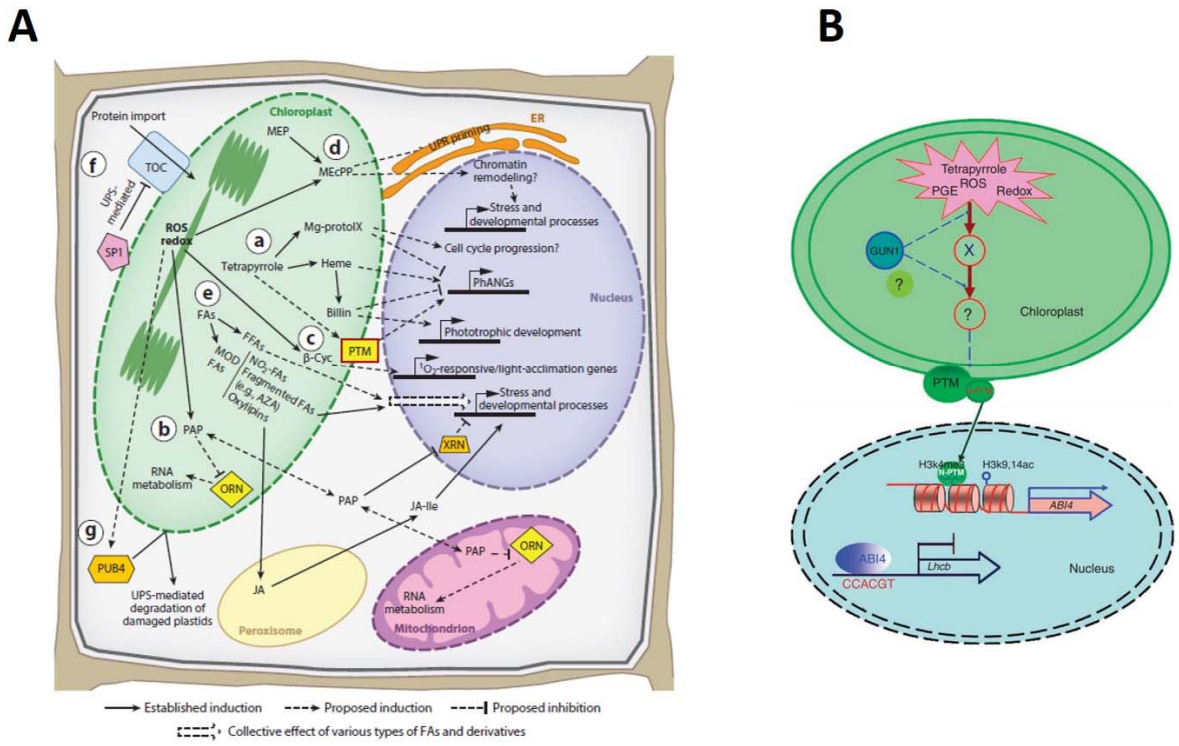

Figure 3: *Retrograde signalling components in plant cells.* ***(A)*** *Confirmed and proposed actions of signalling metabolites in interorganellar communication [Image adapted from de Souza et al 2017].* ***(B)*** *A model showing that PTM acts as sensor/transducer in the retrograde signalling pathways from chloroplasts [Image adapted from Sun et al 2011].*

Mitochondrial retrograde signalling

Mitochondrial retrograde signals have not been well studied in plants (in contrast to those in chloroplasts) but have been extensively studied in yeast and mammalian cells, where they were identified as key regulators of cellular functions [de Souza et al, 2017]. The physiological state of mitochondria can reflect their degree of energy production or O_2 availability, or levels of reactive oxygen species (ROS). These metabolites allow mitochondria to inform the nucleus of these fluctuating conditions, and induce adaptive measures. Not surprisingly, nuclear genes that are related to respiration, peroxisomal biogenesis and oxidative-stress responses are regulated at the

transcriptional level in response to the physiological state of mitochondria [Woodson and Chory, 2008]. The best-studied retrograde signals in plant mitochondria involve increased expression of the nuclear-encoded alternative oxidase (AOX) as an adaptive response to recover from mitochondrial electron transport chain (mtETC) inhibition. AOX reduces the production of ROS, and *Arabidopsis thaliana mitochondrial retrograde regulation deficient (mrrd)* mutants that are unable to induce AOX after mtETC inhibition exhibit ROS-like cellular damage [Woodson and Chory, 2008]. The evidence for the involvement of metabolites in mitochondrial retrograde signaling in plants is not conclusive. However, metabolites such as PAP are potential candidates (**Figure 3 A**), and studies have suggested that the transcription factors NO APICAL MERISTEM/ARABIDOPSIS TRANSCRIPTION ACTIVATION FACTOR/CUP-SHAPED COTYLEDON013 (ANAC013) and ANAC017 are involved in mediating mitochondrial retrograde signals (**Figure 4**) [De Clercq et al, 2013; Ng et al, 2013]. Moreover, Giraud et al. 2009 reported that the function of ABI4 is regulated by both plastidial and mitochondrial signals. Indeed, subsequent studies have identified REGULATOR OF ALTERNATIVE OXIDASE 1 (RAO1) as the nucleus-localized cyclindependent kinase E1 (CDKE1) protein that integrates mitochondrial retrograde signals with energy signals under stress conditions (**Figure 4**). Interestingly, *rao1* mutants are compromised in their response to altered redox and energy status in both chloroplasts and mitochondria, suggesting the key role of CDKE1 in establishing metabolic homeostasis by harmonizing the activities of these two organelles. These results illustrate the exquisite coordination of molecular and metabolic processes that synchronize the activity of these energy-regulating organelles [de Souza et al, 2017].

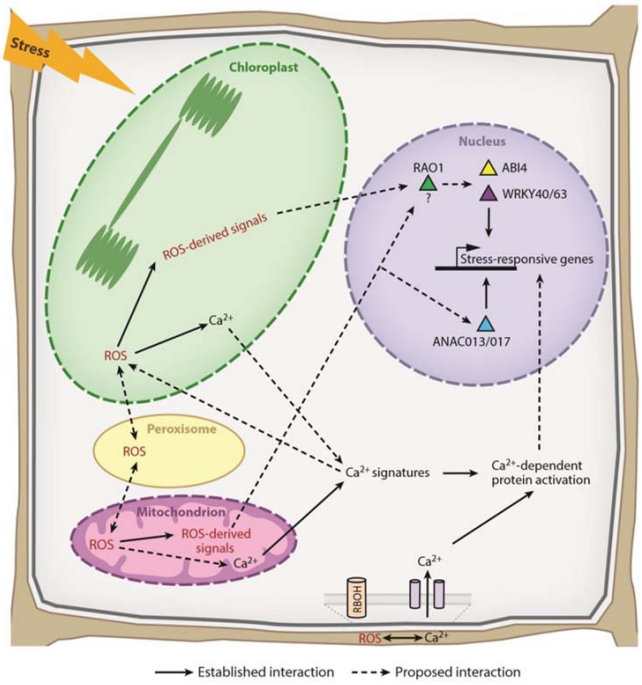

Figure 4: *Retrograde signalling components in plant cells. $Ca^{2+}$and ROS as the master initiators of interorganellar communications. Selected proteins involved in signal strasduction are shown, including RAO1, ANAC013 and ANAC017 and ABI4 [Image adapted from de Souza et al, 2017].*

The family of Whirly proteins

Whirlies form a small family of single-stranded DNA (ssDNA) binding proteins found mainly in the plant kingdom [Maréchal et al 2008]. Although most flowering plants contain two members, some species including Arabidopsis thaliana have three *WHIRLY* genes. In Arabidopsis thaliana, these genes are located on chromosomes I and II (At1g14410, At1g71260 and At2g02740). All three proteins have a putative DNA-binding domain, an oligomerization domain and a target paptide. Critical for the interaction with DNA is a motif consisting of six amino acids, Lys-Gly-Lys-Ala-Ala-Leu (KGKAAL). Mutations in this domain not affect the tetramerization of the protein but abolished DNA-binding activities [Krause et al 2005]. Whirly proteins preferentially bind single-stranded DNA (ssDNA) and perform numerous activities related to DNA metabolism, including the regulation of transcription and modulation of telomere length. Arabidopsis Whirly1 and 3 are required for plastid genome stability [Marechal et al, 2009] and the barley homologue interacts with intron-containing plastidic RNA [Melonek et al, 2010]. In fusion with GFP, the Arabidopsis Whirly1 and 3 proteins were shown to be targeted to chloroplasts, and the Whirly2 was targeted to mitochondria (**Figure 5 A**) [Krause et al 2005]. While an AtWhirly1 was shown to be specifically and efficiently imported only into chloroplasts, AtWhirly2 was translocated *in vitro* into both chloroplasts and mitochondria (**Figure 5 B**) [Krause et al 2005].

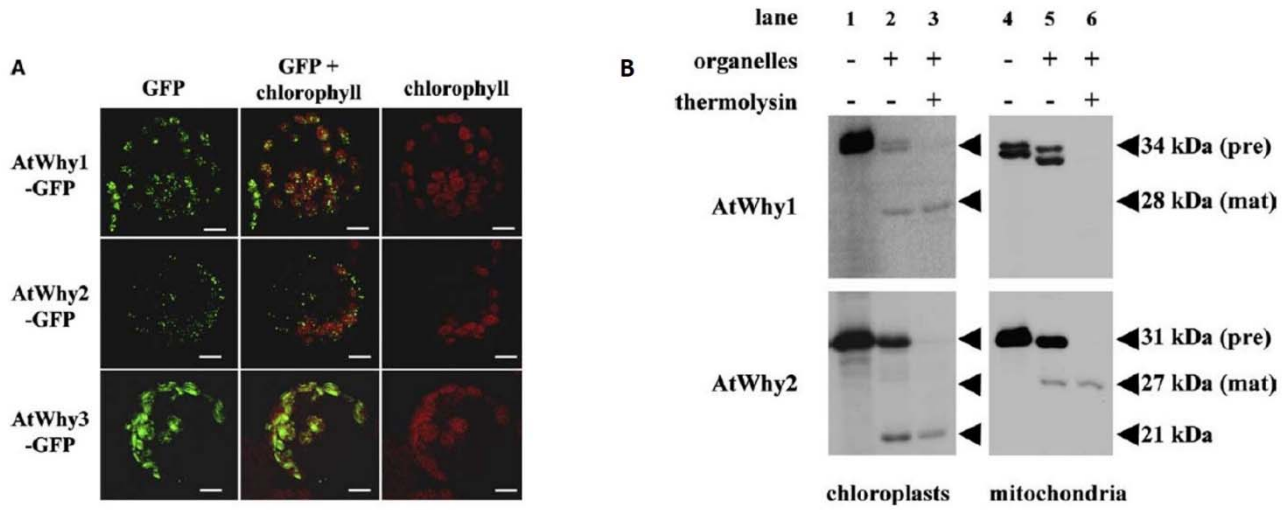

Figure 5: *Subcellular localization of Whirly proteins* ***(A)*** *Subcellular localization of AtWhirly1-GFP, AtWhirly2-GFP and AtWhirly3-GFP fusion proteins in potato protoplasts. Confocal images of GFP fluorescence and chlorophyll autofluorescence are shown in the left and right columns, respectively. The middle column depicts the merged images.* ***(B)*** *In vitro protein import assay of the AtWhirly1 and AtWhirly2 into isolated chloroplasts and mitochondria [Figures adapted from Krause et al 2005]. Precursor proteins were synthesised and labelled in vitro (lanes 1 and 4) and incubated with isolated chloroplasts (lanes 2 and 3) or mitochondria (lanes 5 and 6). Upon termination of the import reaction, half of the assay was incubated on ice in the absence (lanes 2 and 5) or the presence of 20 lg thermolysin (lanes 3 and 6). The sizes for the translated precursor polypeptides (pre) and the processed mature polypeptides (mat) are given on the right [Krause et al 2005].*

The first member of the Whirly family to be functionally identified was p24 (StWhirly1) in *Solanum tuberosum.* It was characterized as a transcriptional activator of the pathogenesis-related gene *PR-10a* following elicitation or wounding of potato tubers. In barley, Whirly1 binds to the promoter of the senescence-associated gene *HvS40*, which is induced during pathogen infection and by senescence as well as by the hormones such as salicylic acid (SA), jasmonic acid (JA) and abscisic acid (ABA), whose synthesis begins in plastids [Foyer *et al,* 2014]. Analysis of the crystal structure of StWhirly1 revealed that *in vivo* Whirlies adopt a tetrameric form. Each protomer consists of two antiparallel β sheets packed perpendicularly against each other forming blade-like extensions which protrude out of an α-helical core that allows formation of a stable tetramer. The surface formed by these "blades" was proposed to form the Whirly ssDNA-binding domain (**Figure 6**) [Maréchal *et al,* 2008].

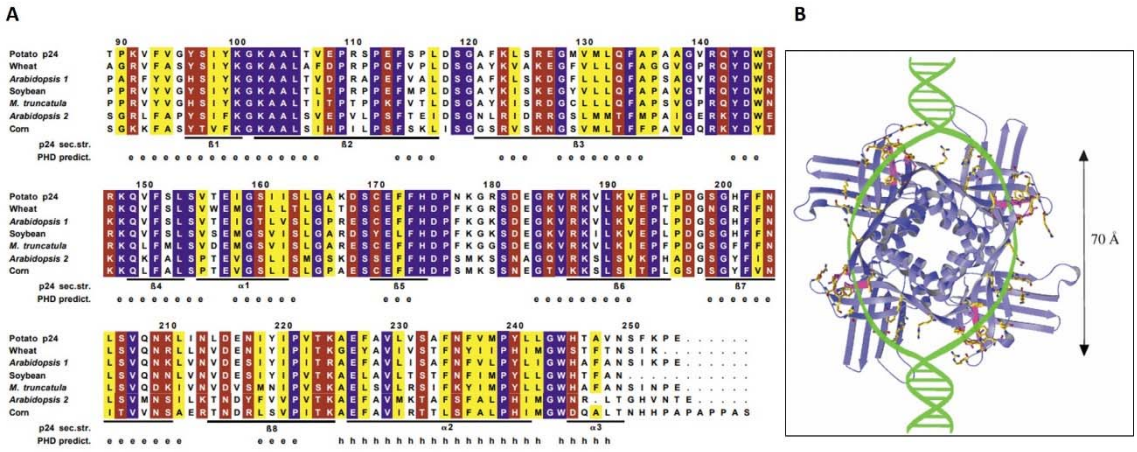

Figure 6: *Structural conservation of Whirly proteins.* ***(A)*** *Sequence alignment of seven Whirly proteins from various plant species.* ***(B)*** *Quaternary structures of Solanum tuberosum p24 protein. P24 can bind melted dsDNA [Figures adapted from Desveaux et al, 2002].*

Recently it was suggested that Whirly1 protein could be involved in the retrograde signalling from chloroplasts to nucleus; indeed, an intriguing feature of Whirly1 is that it is a dual-targeted protein. Dual targeting of proteins is defined when the protein product (or products) of a single gene are targeted to more than one location within the cell [Carrie and Whelan, 2013]. The barley Whirly1 protein is dual localized to both chloroplast and mitochondria [Grabowski *et al,* 2008] with the same molecular weight for both forms. On the other hand, in *Arabidopsis* the Whirly1 protein of the same molecular weight was found in both chloroplasts and nucleus of the same cell [Estavillo *et al,* 2013]. Interestingly, it was shown that recombinant Whirly1 can move from chloroplasts to the nucleus by transformation of tobacco plastids with a HA-AtWhirly1 fusion protein [Isemer *et al,* 2012]. These features of Whirly1 make the protein an ideal candidate for information trafficking from plastids to the nucleus and a model of the Whirly1-dependent perception and transduction of signals was proposed (**Figure 7**) [Foyer *et al* 2014].

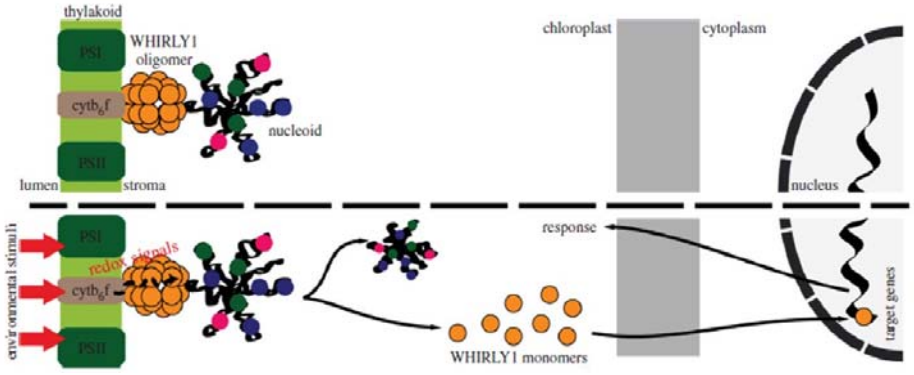

Figure 7: *Schematic model of the Whirly1-dependent perception and transduction of redox signals originating from the photosynthetic apparatus. Under control conditions, Whirly1 forms 24-oligomers which form a bridge between the thylakoid and the nucleoid. In response to environmental stimuli, the redox state of the photosynthetic apparatus is altered and this induces a monomerization of Whirly1. Whirly1 monomers can translocate to the nucleus where they regulate expression of target genes [Figure adapted from Foyer et al 2014].*

Plant mitochondria

Mitochondria are vital organelles that perform a variety of fundamental functions ranging from the synthesis of ATP through to being intimately involved in programmed cell death. Mitochondrial morphology may vary to a great extent between organisms and tissues depending on cell type and physiological state. However, the organelles are typically 1–2 µm long and 0.1–0.5 µm in diameter [Preuten et al 2010]. Comprised of at least six compartments: outer membrane, inner boundary membrane, intermembrane space, cristal membranes, intracristal space, and matrix (**Figure 8**). Although higher-plant mitochondria usually are discrete, spherical organelles, they display high motility and undergo frequent fusions and fissions. Mitochondria have a complex, dynamic internal structure. This internal dynamism is reflected in the pleomorphy and motility of mitochondria. Although mitochondria contain their own genome and protein synthesizing machinery they are only semi-autonomous: the majority of mitochondrial polypeptides are encoded in the nuclear genome, synthesized in the cytosol and imported into the mitochondria post-transcriptionally [Logan 2006].

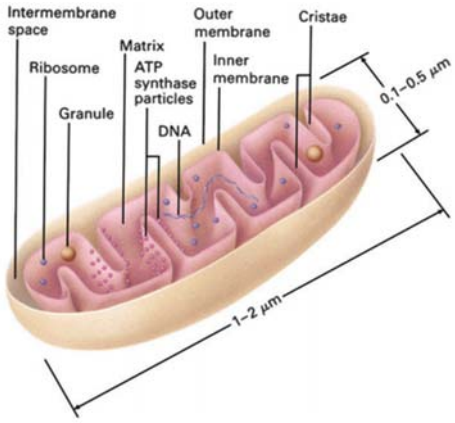

Figure 8: *Mitochondria structure that comprise outer membrane, inner membrane, intermembrane space and matrix [Figure adapted from Frey and Mannella, 2000].*

Flowering plants possess the largest known mitochondrial genomes (chondromes). Whereas mitochondrial genomes of animals range in size from approximately 15–18 kb, and those of fungi from 18 to more than 100 kb, plant chondromes are substantially larger and range from 208 kb in white mustard (*Brassica hirta*) to over 2400 kb in muskmelon (*Cucumis melo*) [Preuten et al 2010]. As most genes identified in the mitochondrial genome are indispensable for mitochondrial function, it is generally believed that each mitochondrion must possess at least one full copy of the genome. Indeed, this seems to be the case in animals. For example, although the number of mitochondria per cell varies in human, mouse, rabbit, and rat cell lines, the mtDNA copy number

per mitochondrion remains constant. Plant cells, however, have very few copies of the mtDNA compared with the number of mitochondria [Cai et al 2015]. Thus, in plant cells, each mitochondrion does not possess one complete copy of the mtDNA, a phenomenon that occurs commonly in somatic cells of plants [Preuten et al., 2010]. In addition, work in *Arabidopsis*, barley (*Hordeum vulgare*), and tobacco (*Nicotiana tabacum*) showed that cells in leaves, stems, and roots contain few copies of the mtDNA (40–160), whereas cells in root tips contain more copies (300–450) [Preuten et al., 2010].

Plant mitochondrial electron transport chain

Photosynthesis and respiration are the primary pathways of carbon and energy metabolism in plants. Photosynthesis uses light energy, CO_2 and H_2O to drive the synthesis of carbohydrates and release of O_2. Respiration then uses these carbohydrates to support growth and maintenance through the provision of carbon intermediates, reducing equivalents and ATP. These processes, in turn, release CO_2 and convert O_2 back to H_2O. Glycolysis, the oxidative pentose phosphate pathway and the mitochondrial tricarboxylic acid cycle are the central respiratory pathways using photosynthesis-derived carbohydrate to supply carbon intermediates for biosynthesis, as well as coupling carbon oxidation with the reduction of NAD(P) to NAD(P)H. These reducing equivalents are then used to support biosynthetic reactions or can be oxidized by the mitochondrial electron transport chain (ETC), localized in the inner mitochondrial membrane (IMM). Complex I (NADH dehydrogenase), as well as a series of other plant-specific “alternative” dehydrogenases couple NAD(P)H oxidation to reduction of the ubiquinone pool. Complex II (succinate dehydrogenase of the TCA cycle) is a further supply of electrons for the ubiquinone pool. Electrons in ubiquinol are then passed to complex III, cytochrome (cyt) c and finally complex IV (cyt oxidase), which catalyzes the four-electron reduction of O2 to H2O. Importantly, electron transport at complexes I, III and IV is coupled with proton translocation from the mitochondrial matrix to inner membrane space (IMS) and the resulting proton motive force is used by complex V (ATP synthase) to generate ATP from ADP and Pi (**Figure 9**). A defining feature of the plant mitochondrial ETC is the presence of two terminal oxidases (**Figure 9**). In addition to cyt oxidase, an alternative oxidase (AOX) is present that directly couples the oxidation of ubiquinol with the reduction of O_2 to H_2O. AOX introduces a branch in the ETC, such that electrons in ubiquinol are partitioned between the cyt pathway (complex III, cyt c, complex IV) and AOX. Notably, AOX dramatically reduces the energy (ATP) yield of respiration since it is not proton pumping and since electrons flowing to AOX bypass the proton

pumping complexes III and IV. Electron flow to AOX can still support a reduced ATP yield if these electrons arise via the proton-pumping complex I. However, if electron flow to AOX is being supported by an alternate dehydrogenase or by complex II (that, unlike complex I, are not proton-pumping), then electron flow will be completely uncoupled from ATP turnover. In summary, plants have additional ETC components that allow for a dramatic modulation of ATP yield depending on the components of the path used for NAD(P)H oxidation and O_2 reduction [Vanlerberghe, 2013].

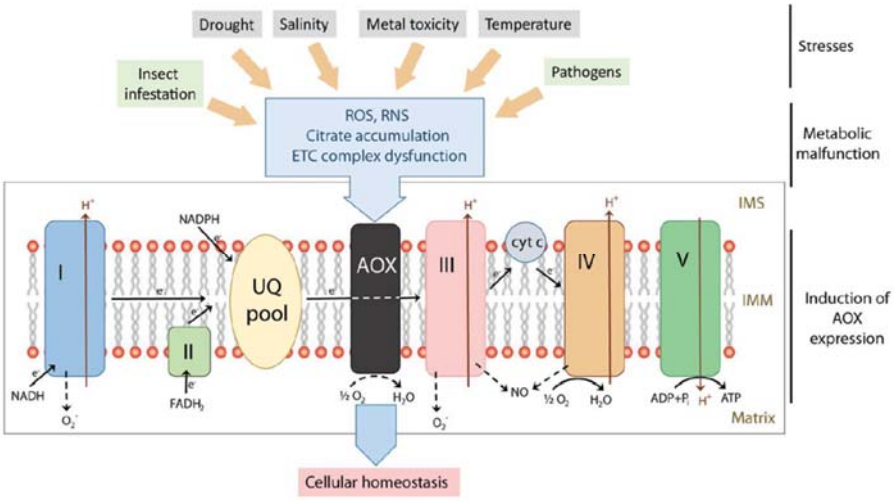

Figure 9: *Plant mitochondria electron transport chain. Alternative Oxidase is highly responsive to abiotic and biotic stress and dysfunctions in respiratory metabolism [Saha et al 2016].*

Alternative oxidase in plants

Plants being sessile, are exposed to various environmental stressors during their life, such as drought, salinity, metal toxicity, low or high temperature, nutrient deficiency and pathogen attack. Alternative Oxidase (AOX) is one of the molecules involved in stress response and mediates a retrograde signaling pathway to architect a tolerance/avoidance response [Saha et al, 2016]. AOXs are interfacial membrane bound, cyanide insensitive, metallo-protein involved in mitochondrial redox reactions [Saha et al, 2016]. The plant AOX is encoded by a small gene family, consisting of two distinct subfamilies termed AOX1 and AOX2. Dicotyledons contain members of both subfamilies while monocotyledons contain only AOX1 genes. Expression of the AOX1 genes is highly responsive to abiotic and biotic stress, as well as dysfunctions in respiratory metabolism. The AOX2 genes are generally not responsive, or at least much less responsive, to such conditions [Vanlerberghe G.C., 2013]. One of the important stimulants is the dysfunction in mitochondrial electron transport chain complexes I, III and IV. Thus any component leading to cytochrome pathway complex dysfunction will lead to induction of AOX [Saha B. et al, 2016].

Complex I in plants

Complex I (NADH–ubiquinone oxidoreductase), the largest protein complex (molecular mass of about 1 MDa) in the plant respiratory chain, is the major entry point of electrons into the oxidative phosphorylation system. *Arabidopsis thaliana* complex I includes at least 49 subunits, 17 of which are unique to plants. The majority of plant complex I subunits have nuclear encoded genes, but nine, *NAD1-7*, *NAD4L* and *NAD9*, are encoded by the mitochondrial genome [Juszczuk I.M. et al, 2012]. Electron microscopy studies have revealed that complex I in *Arabidopsis* is composed of two domains arranged in an orthogonal configuration that forms an L-shaped particle. The membrane arm is hydrophobic and responsible for proton translocation across the inner membrane, and the peripheral arm, involved in electron transfer from matrix NADH to ubiquinone, is hydrophilic and protrudes into the mitochondrial matrix. In mutants with dysfunction or loss of complex I, acclimation and then survival are associated with re-organization of respiratory metabolism. While total respiratory activity might be enhanced, as in the tobacco CMSII mutant, or not significantly modified, as in the *Arabidopsis ndufs4* mutant, the capacities of the alternative pathways are often changed. Overall, these data suggest that plant mutants with altered or no complex I can adapt their respiratory metabolism by inducing alternative pathways of the respiratory chain, and that this has implications for the functioning of the whole cell [Juszczuk I.M. et al, 2012].

AIM OF THE THESIS

Plant cells have three genetic compartments, with the nucleus carrying the largest part of genomic information on chromosomes. Organelles have retained a genome, but present-day organelle genomes are severely reduced and encode few proteins. In fact, most proteins (93-99%) that are found in organelles are encoded in the nucleus, synthesized in the cytoplasm and then imported into the organelle. The compartmentalization of genomes requires a coordination of the gene expression among different subcellular compartments in order to guarantee the correct concentration of organelle proteins and to maintain organelle function [Pfannschmidt, 2010]. This coordination occurs through anterograde and retrograde mechanisms. Retrograde mechanisms have evolved to communicate the functional and developmental state of organelles to the nucleus, which can then modulate anterograde control and cellular metabolism accordingly. Recently was suggested that Whirly1 protein could be involved in the retrograde signalling from chloroplasts to nucleus. *Arabidopsis thaliana* has three Whirly proteins with different subcellular localization: Whirly1 and Whirly3 are targeted to chloroplasts, while Whirly2 is targeted to mitochondria [Krause et al. 2005]. The aim of this PhD project was to elucidate the *in vivo* role of the mitochondrial protein Whirly2, in order to investigate a possible involvement in organelles cross-talk. For this purpose, an *Arabidopsis thaliana* T-DNA insertional mutant for the *WHIRLY2* gene was molecularly and physiologically characterized by comparison with WT plants. We investigated the phenotype of plants at different developmental stages, the role of Whirly2 on mitochondria functionality and morphology and gene expression regulation in different physiological, developmental and stress conditions.

MATERIALS AND METHODS

Plant materials and growth conditions

All experiments were performed using *Arabidopsis thaliana* ecotype Columbia (Col-0). The mutant line for whirly2 (SALK_118900), was obtained from the European Arabidopsis Stock Centre (NASC). The plant seeds were surface sterilized in 70% EtOH and 0.05% Triton X-100, followed by 100% EtOH. The seeds were sown onto square Petri dishes containing one-half-MS medium [Murashige and Skoog, 1962] supplemented with 0.5 g/l MES-KOH, pH 5.7, 0.8% Plant Agar (Duchefa), and different concentrations of sucrose (0% to 3%), stratified for 2 days at 4 °C in the dark, and placed vertically in a growth chamber under a long daylight period (16h light/ 8h dark) using 150 µmol m−2 s−1 at 22 °C. Some experiments were performed on MS medium supplemented with different concentrations of sucrose (0% to 3%). The experiments were conducted at different *Arabidopsis* growth stages, as defined by Boyes et al 2001 (**Figure 10**).

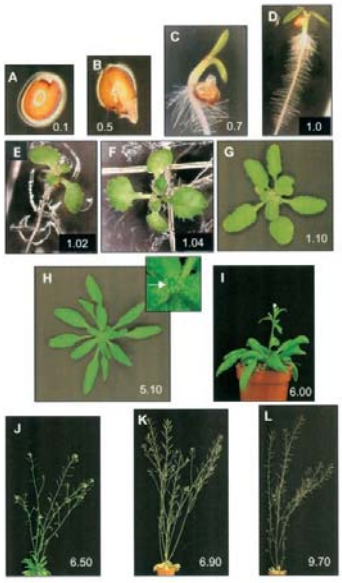

Figure 10: *Arabidopsis growth stages. Image adapted from Boyes et al 2001.*

Some experiments were conducted with non-embryogenic cell suspension cultures of WT and *whirly2 ko.* Suspension cell cultures were grown at 25°C under a long daylight period on a gyratory shaker in liquid MSR2 medium (MS medium; 2 mg/l glycine; 0.5 mg/l nicotinic acid; 0.1 mg/l thiamine hydrochloride; 0.5 mg/l pyridoxal hydrochloride; 100 mg/l myo-Inositol; 0.5 g/l malt extract; sucrose 3%; 1 mg/l 6-BAP; 2 mg/l 2,4-D; pH 5.7). For subculturing, two ml of packed cells

were transferred into 50 ml fresh medium every week. To determine the growth capabilities of the two suspension cell cultures lines, cells were filtered and the fresh and the dry weight were measured. For the dry weight, the cells were placed in a stove for 24 hours at 40°C. Experiments were performed at 5 days after sub-cultivation, when cells are on exponential growth phase.

Cell viability

Cell death accompanying the loss of membrane integrity was evaluated by a spectrophotometric assay of Evans blue stain retained by cells according to Gaff and Okong'o-Ogola (1971) with minor modifications. One ml of cell suspension was sampled from the cultures at different days after subculture. Evans blue dye solution was added to the cell suspensions to a final concentration of 0.05% and incubated for 20 minutes at room temperature, followed by excessive washes with water until the washing showed no significant blue colour. The washed cells were then added to 50% methanol containing 1% (w/v) sodium dodecyl sulfate (SDS) and incubated at 55 °C for 30 min. Absorbance of the supernatant was measured spectrophotometrically at 600 nm. The resulting OD was compared to the absorbance of cells boiled for 15 minutes, which are considered as 100% dead.

Antimycin and spectinomycin plant treatment

Plant were growth on MS 1,5% sucrose supplemented with 50 µM of antimycin (Sigma-Aldrich) or 50 mg/l of spectinomycin (Sigma-Aldrich). Plants were grown under long day conditions as reported previously. Samples were separately collected at 1.04 stage of growth and frozen at -80°C, for subsequent analyses.

Germination and plant growth analyses

The images were captured using a stereomicroscope (Leica MZ16F) in order to analyzed seeds size, germination and plant growth at different days after sowing (das). Different media compositions were tested. For root growth assay, the plant seeds were sown onto solid growth medium (MS-1/2 1% sucrose), vertically grown as described above and scanned using a flatbed scanner. The images were analyzed through image analysis (Fiji – ImageJ bundle software). The experiments were performed at least three times and each sample comprised 25 seedlings.

Tetrazolium assay for seed viability test

Tetrazolium (2,3,5 triphenyl tetrazolium chloride, TZ) assay is the fast evaluation for seed viability. The brief description of this protocol has been reported in Verma *et al.*, 2013.

1. Scarify the *Arabidopsis* seeds by soaking approximately 100 seeds (in three replicates) in 1 ml scarification solution (20 ml commercial bleach and 100 µl Triton X-100 in 100 ml autoclaved distilled water) for 15 min under shaking conditions at room temperature. Wash at least five times with distilled water to remove the bleach.
2. After scarification, remove excess water and incubate the seeds with 1% TZ solution at 30°C for 24 to 48 h in dark (observe the seeds after 24 h and proceed with step 3 if stain appears). Take heat killed (100 °C, 1 h) seeds as negative control.
3. After staining, wash the seeds 2-3 times with distilled water.
4. Observe the seeds under stereo microscope.
5. Evaluate the seeds on the basis of staining pattern and colour intensity. Among stained seeds, seeds with bright red staining are completely viable while partially stained seeds may produce either normal or abnormal seedlings. Pink or greyish red stain indicates dead tissue. Completely unstained seeds are non-viable.

Oxygen consumption Measurements

Oxygen consumption was measured using a Clark-type oxygen electrode (Hansatech Instrument). Respiration on of *Arabidopsis* suspension cell cultures was measured in the dark at 25°C. 1 ml of 5 days suspension cell cultures was placed in the chamber containing 1 ml of MSR2 medium. Oxygen consumption was measured for at least 5 minutes before the addition of 1 mM KCN or rotenone.

TMRM Staining

Cells and seedlings were incubated for 20 minutes in 0,5 µM of TMRM solution. Samples were washed twice (10 mM MES, 10 mM $CaCl_2$, 5 mM KCl pH 5.8) and then observed. The images were acquired using the ZEISS LSM700 laser scanning confocal imaging system (535 nm excitation; 600 nm emission). High-definition images were acquired (1024×1024, 65× objective) and analyzed using the Fiji – ImageJ bundle software (http://fiji.sc/Fiji). The experiments were performed at least in triplicate, and each sample set comprised 10 samples.

Transmission electron microscopy (TEM)

TEM analyses were performed in WT and *whirly2 ko Arabidopsis* cells at 5 days after subcultures. The cells were fixed in 6% gluteraldehyde and conserved at 4 °C. Subsequently, the samples were centrifuged for 3 minutes at 2000 rpm and fixed in OsO_4 1 M in 0.2 M cacodylate buffer pH 6.9. The samples were placed for two hours in the dark at room temperature. Osmium was removed by centrifugation (3 minutes at 2500 rpm), than the dehydration phase was carried out with 3 washings of 10 minutes for each concentration of ethanol (25%, 50%, 75%). Finally, 3 washes of 20 minutes were performed with 95% ethanol. Subsequently, three 5-minute washes were carried out with propylene oxide. For the inclusion phase, multi-component Durcopan epoxy resins were employed (27 ml of AM araldite + 23 ml of dodecyl-succinic DDSA anhydride) and a polymerizing agent was added. Different proportions of propylene oxide:resin were used:

- ratio 3:1, stove at 40°C for 1 hour;
- ratio 1:1, stove at 40°C for 1 hour;
- ratio 1:3, stove at 40°C for 1 hour;
- 100% resin, stove at 40°C over night and 60°C for three days.

The included samples were cut with a diamond blade in ultra-thin sections using the ultramicrotome Reichert Ultracut S (Reichert). The obtained sections were contrasted with uranyl acetate and lead citrate. The sections were observed with an transmission electron microscope FEI Tecnai 12 (Philips).

RNA isolation and qRT-PCR

Plants and cells of wild-type (WT) and *whirly2 ko* were harvested for subsequent analyses. Total RNA was extracted from samples using RNeasy® Plant Mini Kit (Quiagen) according to the manufacturer's instructions. RNA concentration was measured using a Nanodrop ND-1000 spectrophotometer (Nanodrop Technologies, Rockland, DE, USA). First-strand cDNA synthesis was performed using 1 µg of RNA, oligo(dT) primers, and SuperScript-II Reverse Transcriptase (Invitrogen) according to the manufacturer's instructions. The qRT-PCR reactions were performed with 100 ng of cDNA using the SYBR Green technology of Go Taq®qPCR Master Mix (Promega) in a 7500 Real-time PCR System (Life Technologies). The primers sequences for qRT-PCR are reported in **Table 1**. The expression levels of each gene were normalized to the expression level of the

housekeeping gene Actin-2 (ACT2; At3g18780) and analyzed using the ΔΔCT method [Livak and Schmittgen, 2001].

DNA isolation

The samples were first grinded in liquid nitrogen and then added to 500 µl of extraction buffer (100 mM Tris HCl pH8; 500 mM NaCl; 50 mM EDTA pH8). Samples were incubated for 5 minutes at 65°C after the addition of 35 µl of SDS 20%. 130 µl of potassium acetate 5M were added to the samples and incubated for 5 minutes in ice. Samples were centrifugated at full speed for 10 minutes and the supernatant was transferred in a new tube containing 500 µl of cold isopropanol, incubated at -20°C for 10 minutes and then centrifugated at full speed for 10 minutes. The pellet was washed twice with 500 and 150 µl of 70% EtOH, air-dried and resuspended in 50 µl of sterile water. DNA concentration was measured using a Nanodrop ND-1000 spectrophotometer (Nanodrop Technologies, Rockland, DE, USA).

Copy number quantification

Total DNA was isolated from plant material, and subsequently treated with an RNaseA at 37°C for 30 minutes. The RNase was removed by DNA precipitation using 2.5 volumes of ice cold 96% EtOH and 0.1 volume 3M sodium acetate. The qPCR reactions were performed in a 7500 Real-time PCR System (Life Technologies) with 50 ng of total DNA using the SYBR Green technology of Go Taq®qPCR Master Mix (Promega). All DNA quantifications were normalized to the amount of the nuclear encoded single-copy gene *RpoTp* as internal standard using the ΔCt method. For the mitochondrial copy number quantification *atp-1* was used as target gene. For the plastidial copy number quantification *psbC* was used as target gene. Primer sequences are reported in **Table 1**.

Primer list

Sequences of primers used in this work are reported in the table:

Table 1: *Primer list.*

Primer Name	**Primer Sequence**
act2_fwd	AAGCTCTCCTTTGTTGCTGTT
act2_rvs	GACTTCTGGGCATCTGAATCT
why1-fwd	ACTTCGAGAAGCAGAGGTTCGG

why1-rvs	TCTAGCAGGCAATCCTTCAGCAG
why2-fwd	GCATCCTCAAAACCAATGAC
why2-rvs	CATGATGTGTGGAAGAGCAA
why3-fwd	ACGATAGAACCACGAGCACCAG
why3-rvs	TGTCAGCTTGAACGCACCAGATTC
ANAC013-fwd	ACCAGACAGATAAACAATGGATCA
ANAC013-rvs	CAGAAGGAACAGGGTTTAGGAA
AOX1a_RT-fwd	TGGTTGTTCGTGCTGACG
AOX1a_RT-rvs	CACGACCTTGGTAGTGAATATCAG
cab1-fwd	TGCACTACTCAACCTCAATGGC
cab1-rvs	AAAGCTTGACGGCCTTACCG
RbcS-fwd	GAAGCTTGGTGGCTTGTAGG
RbcS-rvs	ACCTTATCCGCAACAAGTGG
PolIA-fwd	TTCCGGCGTCAAAGTCACGTGC
PolIA-rvs	TGCACTTCCCTGGACTGGAGTGT
PolIB-fwd	CCTGAATACCGTTCACGTGCCCA
PolIB-rvs	AGCCGCACTTCCCTGAACAGGA
psbC-fwd	CTACCACGTGGAAACGCTCT
psbC-rvs	ATACGATTAATCCGGCATGG
AtRpoTp-fwd	TGGAAGCCGTCTGCTAGAACTA
AtRpoTp-rvs	TGTCTGAATGCAGGTCGAAAC
q-atp1-fwd	CTTAGAAAGAGCGGCTAAACGA
q-atp1-rvs	GGGAATATAGGCCGATACGTCT

Statistics

All experiments were performed at least in three technical and biological replicates. The values are represented as the means ± standard deviation or confidence interval ($p<0.05$). The statistical significance was demonstrated using Student's t-test method.

RESULTS AND DISCUSSION

Plant organelles produce retrograde signals to alter nuclear gene expression in order to coordinate their biogenesis, maintain homeostasis, or optimize their performance under adverse conditions [Estavillo et al 2013]. Retrograde signalling has therefore attracted much research attention aimed at improving understanding of nature of these communication signals [da Souza et al 2017]. Among the putative retrograde signalling molecules, Whirly1 is a candidate for the cross-talk from chloroplasts to nucleus. Whirly1 belongs to a small family of three proteins (called Whirly1, Whirly2 and Whirly3) with a characteristic secondary structure, a conserved DNA binding domain and a different subcellular localization [Desveaux et al 2002]. While large information is available about Whirly1, little is known about the role of the mitochondrial protein Whirly2. Therefore, the aim of this PhD project was to elucidate the *in vivo* role of Whirly2, to investigate a possible involvement in organelles cross-talk. For this purpose, the *Arabidopsis* insertional mutant for *WHIRLY2* gene (*whirly2 ko*) was compared to WT. We investigated the phenotype of mutants at different growth stages, the role of Whirly2 on mitochondria and gene expression regulation in different physiological, developmental and stress conditions.

WHIRLY2 gene is mostly expressed in imbibed seeds

The expression profile of *WHIRLY2* is modulated in different plant tissues and during the plant growth. The Arabidopsis eFP Browser from the AtGenExpress Consortium [Winter et al, 2007] shows that the predicted *WHIRLY2* gene expression is higher in 24 h imbibed seeds and in organs with high degree of cell division such as shoot apex (**Figure 11**).

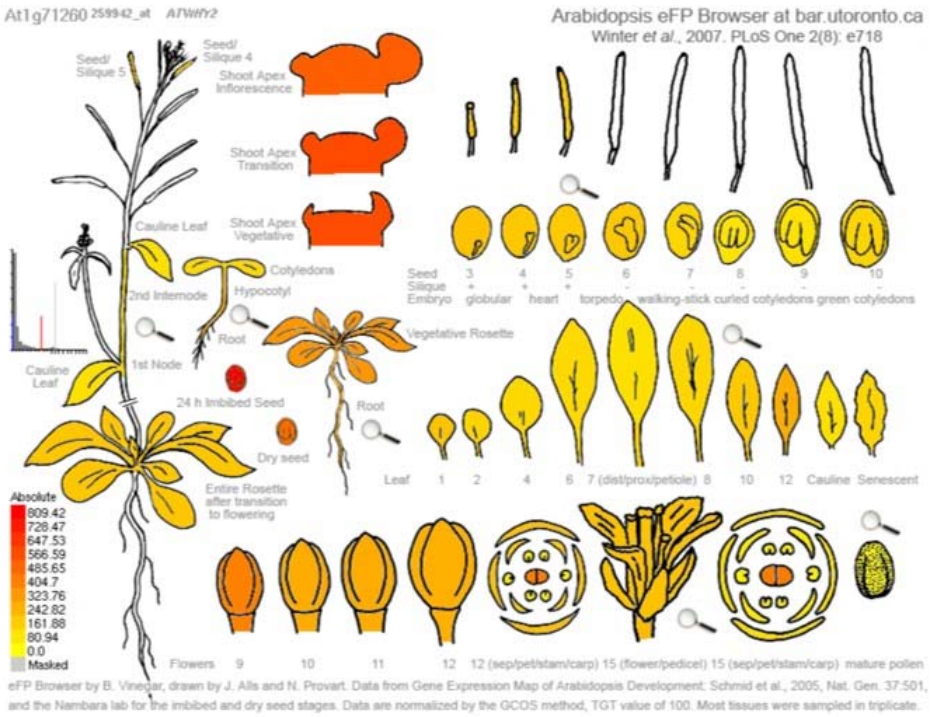

Figure 11: *Arabidopsis eFB browser report showing predicted WHIRLY2 gene expression in different plant tissues. Expression of WHIRLY2 is higher in 24 h imbibed seed, however, expression remains relatively high even in shoot apex [Winter et al, 2007].*

We analysed the expression level of *WHIRLY* genes in our system. The expression of genes in WT was examined in 24 h imbibed seeds and in plants at 1.02, 1.04, 1.10 and 6.00 stages of growth (See Materials and Methods) [Boyes et al 2001]. Ours results reveal that in imbibed seeds the fold change of *WHIRLY2* expression is 1,3 compared to plants at 1.02 stage (**Figure 12**). Conversely, the other two *WHIRLY* genes are less expressed in seeds compared to plants (**Figure 12**). Moreover, in seedlings the highest expression of *WHIRLY* genes was observed at 1.02 stage (**Figure 12**). While the expression of *WHIRLY2* is quite linear during the growth, the expression of *WHIRLY1* and *WHIRLY3* gradually decrease. Many genes encoding proteins localized in chloroplasts, mitochondria, or both organelles, are differentially expressed during leaf and root development. Except for genes encoding photosynthesis-related and chloroplast proteins in leaves, the majority of genes encoding organellar proteins shows a decreased expression level when cells transition from cell proliferation to cell expansion. This trend suggests an key role for mitochondria in delivering cellular energy to support cell proliferation during early organ development and a role for chloroplastic photosynthesis in the production of carbon sources later during development [Van Dingenen et al. 2016]. Our results show how the expression of *WHIRLY* genes is modulated during different stages of growth. In particular, we observed that *WHIRLY2* is highly expressed in

24 hours imbibed seeds and in the early stages of plant growth. Therefore, we investigated about the role of Whirly2 on seeds.

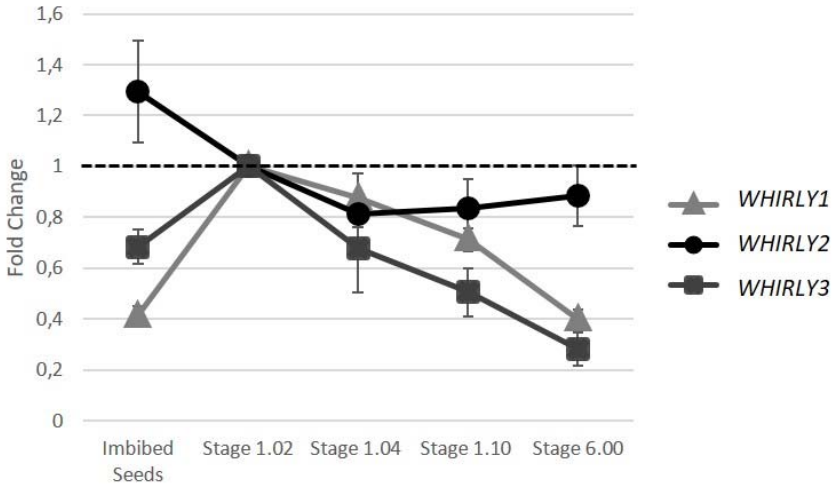

Figure 12: *Expression profile of WHIRLY genes in WT plants and seeds. The expression was analysed in 24 hours imbibed seeds and in plants at 1.02, 1.04, 1.10 and 6.00 stages of growth. The expression was measured in the entire plant (shoot and root), growth on MS-1/2 1% sucrose medium at long day conditions. Data were analyzed using the ΔΔCT method (1.02 seedlings expression=1). Values represent the mean ± confidence interval (p<0.05) of three independent experiments performed in triplicate.*

Whirly2 affects embryo development and seeds viability and germination

We investigated about the impact of Whirly2 protein on seeds. Firstly, we analyzed the seed size which is an important trait in agriculture. The size of a seed is determined by a complex cross-talk from different regions: seed coat, endosperm and embryo. We observed that *whirly2 ko* shows a reduction of seed size around 12% compared to WT (**Figure 13 A and B**). In addition, we noted that approximately 14% of *whirly2 ko* seeds appear deep brown, small and with an irregular shape (**Figure 13 A and C**). The embryos of these seeds are aborted and they did not complete their development. In *whirly2 ko* embryos abortions can be also observed into mature siliquae, indicated by the red stars in the **Figure 13 D**. Together, our results suggest a key role of Whirly2 in embryo development.

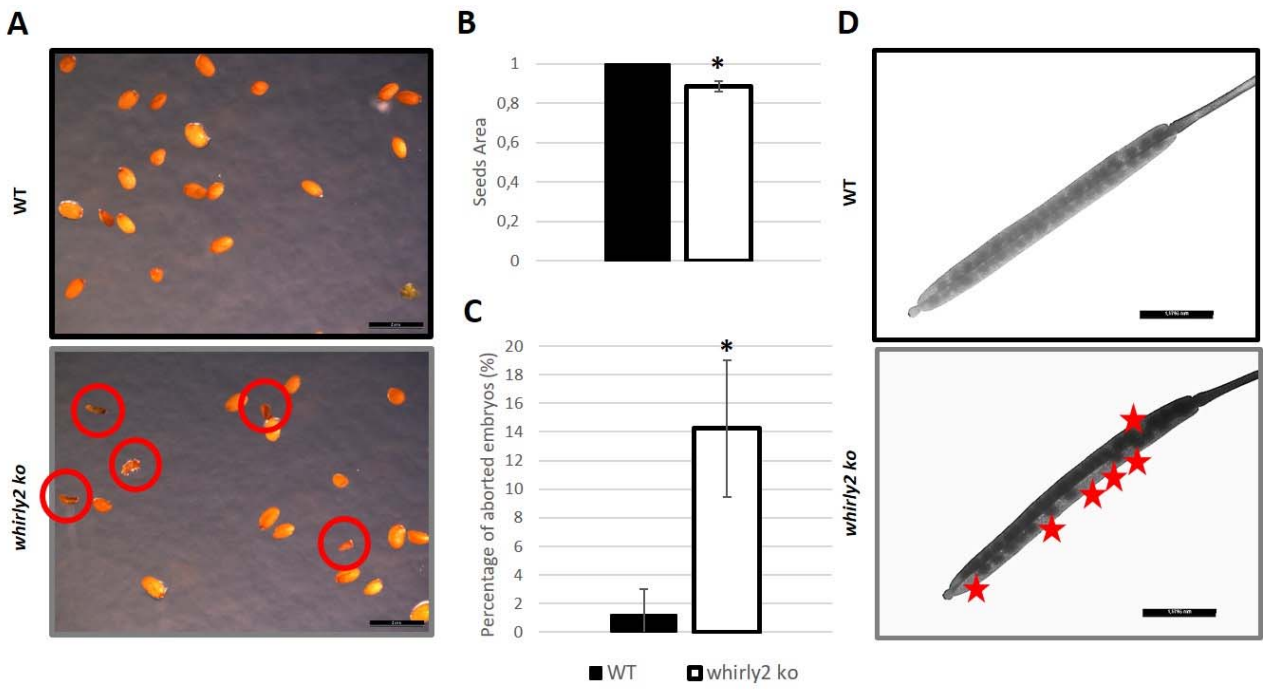

Figure 13: *Comparison between whirly2 ko and WT seeds and siliquae.* ***(A)*** *Stereomicroscope images of dried seeds. Red circles indicate seeds with aborted embryos.* ***(B)*** *Seed area quantification.* ***(C)*** *Percentage of aborted embryos in WT and whirly2 ko.* ***(D)*** *Stereomicroscope images of mature silique of WT and whirly2 ko. Abortions are indicated by red stars. Values reported in the histograms represent the mean ±confidence interval (p<0.05). n=200. *=significant difference between whirly2 ko and WT. The significance was calculated using the Student's test method.*

In higher plants, seed size is a crucial agricultural trait. How plants determine their seed size is also a fascinating question in developmental biology. In angiosperms, seed development begins with a double-fertilization event, which results in the formation of a diploid embryo and a triploid endosperm. Angiosperm seeds comprise three clearly defined components, the embryo, endosperm and seed coat, with each having a distinct genetic composition, which exerts different influences on seed development. Complex cross talk and integration of signals from these different regions together determine the final size of seed [Doughty et al 2014]. In recent years, several signalling pathways of seed size control have been identified in *Arabidopsis* and rice, such as the IKU pathway, the ubiquitin–proteasome pathway, G-protein signalling, the mitogen-activated protein kinase signalling pathway, phytohormones and transcriptional regulatory factors [Na and Yunhai, 2016]. Recently, Meng et al, 2017 proposed a model where normal sugar content controls normal cell elongation for seed size regulation, via a sugar-specific *AN3–YDA* gene cascade. However, the pathways reported in literature are full of gaps, and the interactions between different pathways are largely elusive. Although the mechanism of action of Whirly2 in seeds is far from clear, our results suggest a crucial importance of the protein both for embryo development and seed size determination. One major challenge in the future is to fully elucidate

the molecular mechanisms of seed size control and understand the role of Whirly2 in these pathways.

Mature seeds are an ultimate physiological status that enables plants to endure extreme conditions such as high and low temperature, freezing and desiccation. Seed longevity, the period over which seed remains viable, is an important trait not only for plant adaptation to changing environments, but also, for agriculture and conservation of biodiversity [Sano et al 2016]. We observed an interesting alteration of *whirly2 ko* seed viability. By tetrazolium assay, we calculated that *whirly2 ko* seeds have a reduction in viability of 10% compared WT (**Figure 14**).

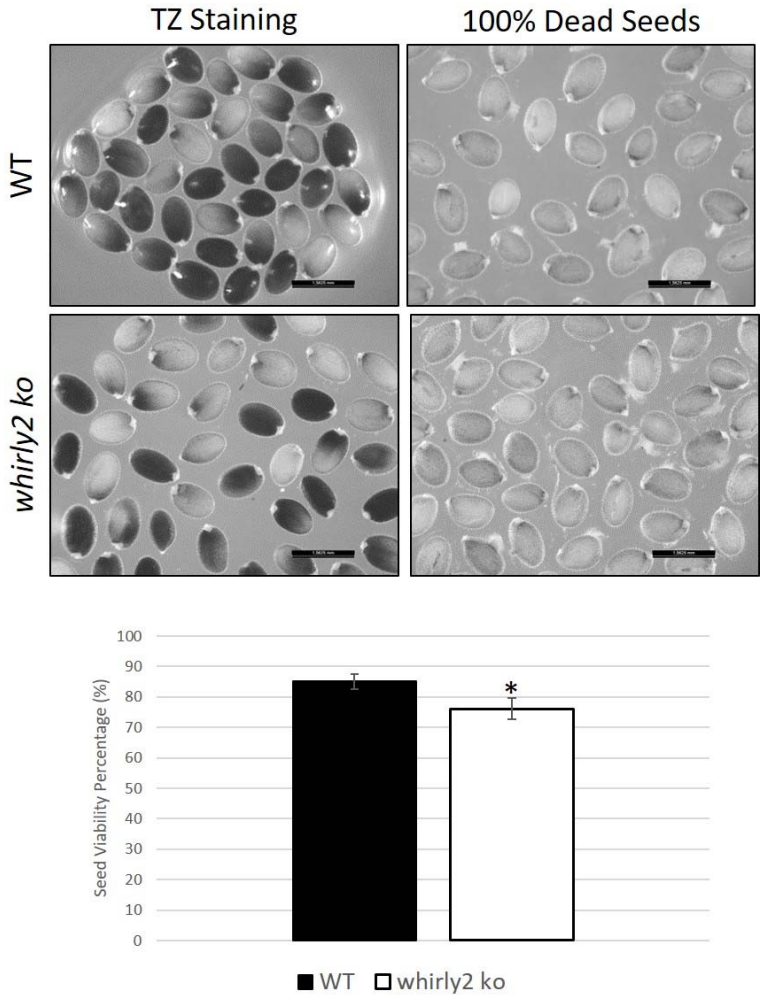

Figure 14: *Tetrazolium seeds viability assay of WT and whirly2 ko seeds. All respiring tissues are capable of converting a colourless compound, TZ to a carmine red coloured water-insoluble formazan by hydrogen transfer reaction catalysed by the cellular dehydrogenases. TZ enters both living and dead cells but only living cells catalyse the formation of formazan which being non-diffusible stains the viable seeds red whereas the absence of respiration prevents formazan production making the dead seeds (aged tissue) remain unstained. Values reported in the histogram represent the mean ±confidence interval ($p<0.05$) of three technical replicas (each includes at least 100 seeds). *=significant difference between whirly2 ko and WT. The significance was calculated using the Student's test method.*

An important aspect for seeds is their ability to germinate under favourable conditions. Seed germination begins with dry mature seed imbibition and ends with radicle protrusion. The most crucial factor for successful germination is selection of the proper environmental condition to initiate this process. Germination depends on regulation of phytohormones, such as gibberellic acid (GA), abscisic acid (ABA), ethylene, and auxin. Environmental factors, including light, temperature, and soil water content and nutrient, influence seed germination mainly through regulating the metabolism and signalling pathways of GA and ABA [Han and Yang, 2015]. Meanwhile, there are drastic morphological changes during seed germination, a tiny seed transforming into a normal seedling, which implies a large-scale changes and regulation of gene expression.

To understand whether the lack of Whirly2 influences this process, we calculated the percentage of germinated seeds. The seeds were sown onto plates with MS-1/2 medium and vernalized at 4°C for 48 hours in the dark. Being sugars known to influence germination and seedling development [Borisjuk et al, 2002], we added two different concentrations of sucrose in the medium: 0% and 1%. The percentage of germinated seeds was calculated both in WT and *whirly2 ko* at 4 days after sowing (das). We considered as germinated a seed after the testa rupture. As can be seen in the **Figure 15 A**, there is a clear difference between the two genotypes. Interestingly, *whirly2 ko* shows a significant reduction in percentage of germinated seeds compared to WT in both sucrose concentrations analysed (**Figure 15 B**). Intriguingly, while WT growth is not influenced by sucrose content, we noted that around 45% of *whirly2 ko* seedlings show a delayed growth with 1% of sucrose (**Figure 15 A and C**). We defined as “delayed growth” a seedling whose length was lower than the average length of the WT seedlings minus the standard deviation value.

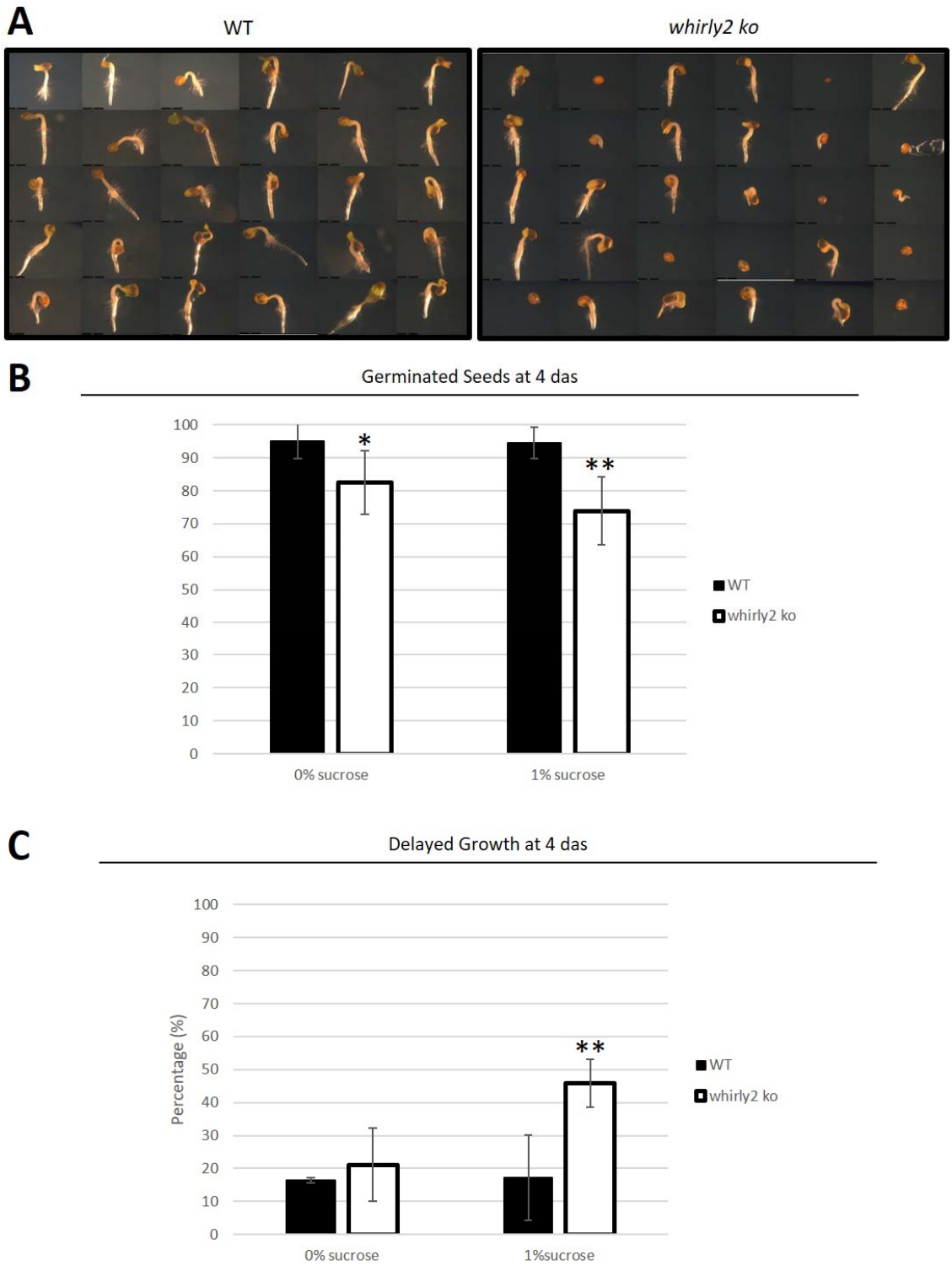

Figure 15: *Comparison between WT and whirly2 ko at 4 das.* ***(A)*** *Stereomicroscope images of WT and whirly2 ko seedlings germinated on MS-1/2 1% sucrose medium.* ***(B)*** *Percentage of germinated seed of WT and whirly2 ko with different sucrose concentrations.* ***(C)*** *Percentage of seedlings with delayed growth. Experiments were performed in MS-1/2 medium with 0% and 1% of sucrose. Values reported in histograms represent the mean ± confidence interval ($p<0.05$) of two independent experiments performed in triplicate. The asterisks indicate values that are significantly different from WT cells using the Student's t test method (* $p<0.05$; ** $p<0.01$).*

Our results suggest a significant role of Whirly2 in seed germination and in seedling establishment.

Seed germination is regulated by very complicated network of signalling and gene expression

regulation. After maturation, the seed is subject to a desiccation stage, a bridge between maturation and germination. The desiccation could lead to damages on membrane system, proteins, and DNAs, which will be more severe along with the fast water absorption upon imbibition [Weitbrecht et al 2011]. To cope with the damages imposed during desiccation and rehydration, plant seeds have evolved fine repair mechanisms on proteins and DNA breaks during imbibition. Membrane system and organelles are also subjected to a repair process upon imbibition. Mitochondria play a key role during in the first phases of plant growth, they exist in mature dry seed but are poorly differentiated. Pre-existing mitochondria are developed and activated in starchy seeds during germination, while more new mitochondria are produced in oil-storing seeds. Mitochondria differentiation process in rice embryo during germination was observed by electron microscope. This differentiation process coincides with the transcript abundance increase of mitochondria proteins, including TCA cycle and respiratory chain related proteins [Howell et al, 2006]. Moreover, several mitochondrial inner membrane import components are essential for seed viability in *Arabidopsis*, consistent with their relatively high levels of transcript abundance during germination. It has been reported that genes peaking in expression during germination are enriched in mitochondrial proteins, particularly those encoding RNA processing functions such as the mitochondrial pentatripeptide repeat (PPR) containing proteins. Thus, the high expression of several inner membrane import components during seed germination supports the findings that a loss-of-function of these results in an embryo lethal phenotype [Murcha et al 2014]. As reported previously (**Figure 12**), the expression of *WHIRLY2* gene is higher in WT imbibed seeds, the first phase of germination. Since Whirly2 localised into mitochondria, hypothetically it can be involved in mitochondria development and activation during germination. Based on our results, we suggest an interesting role of Whirly2 in seed biology, even if other experiments are necessary to unravel the role of the protein in the complex network of signals that regulate seed germination in *Arabidopsis.*

Nutrient availability, particularly of carbon and nitrogen, is one of the most important factors for regulating plant metabolism and development. As previously mentioned, *whirly2 ko* growth is negatively influenced by the presence of 1% of sucrose (**Figure 15 C**). Moreover, we observed that the primary root length is affected in *whirly2 ko* with 1% of sucrose. In particular, the mutant shows a reduction in primary root length of 10% compared to WT at 7 das (**Figure 16**). C-status controls many aspects of plant development, including root growth [Lastdrager et al, 2014]. Sugars

are long-distance signals and there are sugar-dependent regulatory networks in roots [Osuna et al. 2015]. Our results led us to better investigated the effects of nutrients on the mutant.

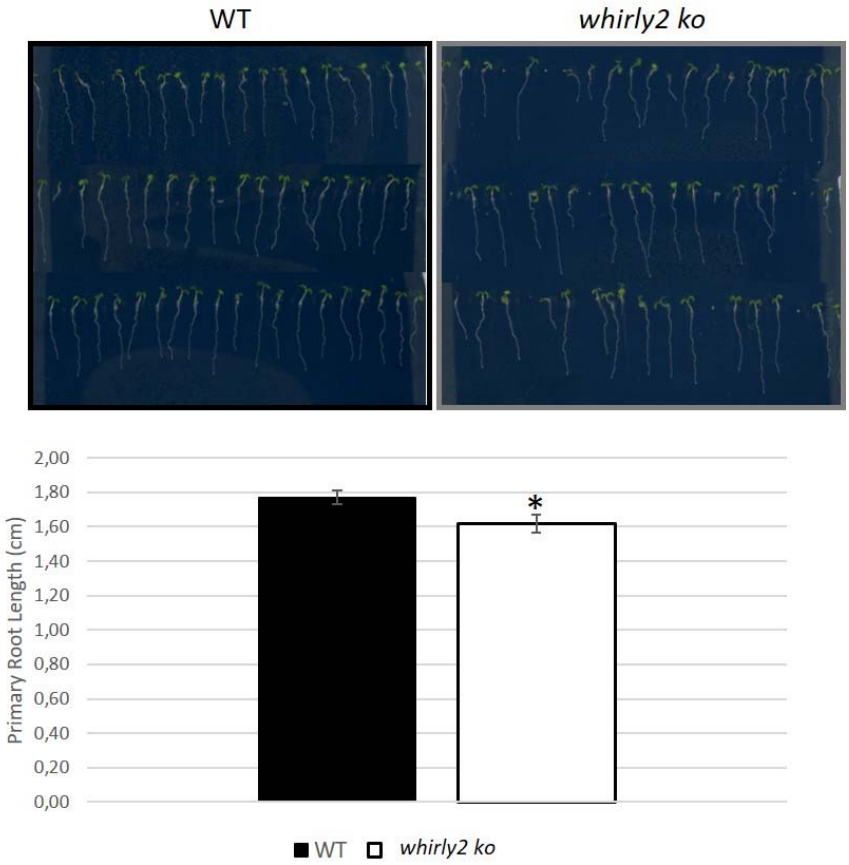

Figure 16: *Measurement of the primary root length in WT and whirly2 ko seedlings at 7 das. Seedlings were sown on MS-1/2 1% sucrose. Values reported in histograms represent the mean ±confidence interval ($p<0.05$) of the root measure of 300 plants for each genotype. *=significant difference between whirly2 ko and WT. The significance was calculated using the Student's test method.*

The percentage of delayed growth seedlings was calculated at 7 das both in WT and *whirly2 ko* germinated on media with different nutrient supply. In particular, we tested two concentrations of sucrose (0% and 3%) in MS-1/2 and MS media. The MS medium contains a double concentration of nutrients respect to MS-1/2, including nitrogen. In MS-1/2 medium WT is affected by 3% of sucrose, indeed the percentage of seedlings with delayed growth is double compared to 0% (**Figure 17**). It is known that the effect of sugars results from a change in the balance between sugar and nitrogen availability rather than sugar abundance alone [Sato et al, 2009]. Conversely, we did not observe any effect of sucrose concentration in *whirly2 ko* (**Figure 17**). When nutrient content increase (MS medium), WT growth retardation percentage is around 20% and no effects were observed between 0% and 3% of sucrose (**Figure 17**). Interestingly, *whirly2 ko* delayed growth is rescue in MS medium with 3% of sucrose compared to 0% (**Figure 17**), suggesting a different response to nutrient availability between WT and *whirly2 ko*.

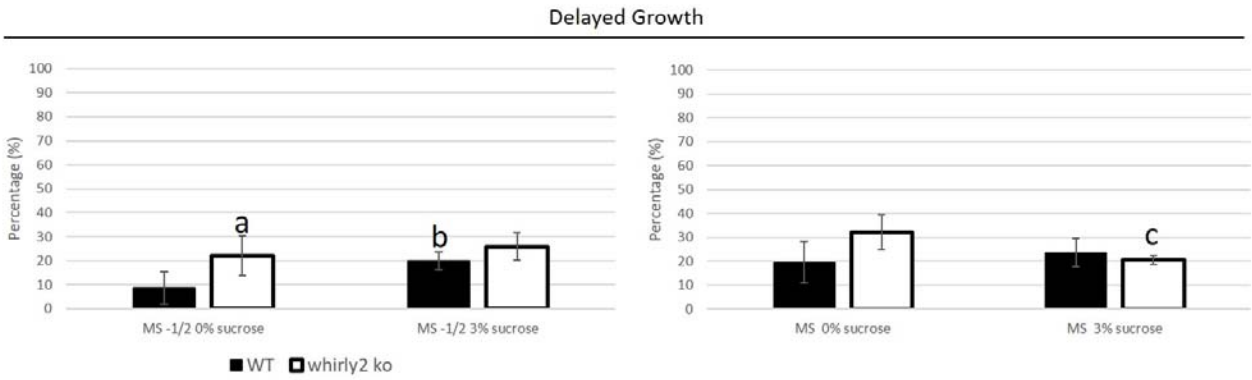

Figure 17: *Effect of C/N balance on WT and whirly2 ko growth. Seedlings were germinated on concentrations of 0% and 3% of sucrose in MS-1/2 and MS media. Seedlings at 7 das were analysed. Values reported in histograms represent the mean ±confidence interval ($p<0.05$) of three independent experiments performed in triplicate ($n=50$ for each experiment). (a=significant difference between whirly2 ko and WT; b= significant difference between WT with different sucrose concentration; c=significant difference between whirly2 ko with different sucrose concentration). The significance was calculated using the Student's test method.*

To their essential role as substrates in energy metabolism and polymer biosynthesis, sugars have important hormone-like functions as primary messengers in signal transduction. Sugar levels regulate the expression of genes involved in diverse physiological and developmental processes throughout the plant life cycle, including germination, early seedling development, morphogenesis, flowering, senescence and various stress responses [Sato et al, 2009]. It is known that sugar-responsive pathways exhibit crosstalk with nitrogen-responsive pathways. Plants are able to sense and respond to changes in the balance between carbon (C) and nitrogen (N) metabolite availability, known as the C/N response. During the transition to photoautotrophic growth following germination, growth of seedlings is arrested if a high external C/N ratio is detected [Sato et al, 2009]. C/N signalling system are influenced by the biological context such as cell-type, developmental, metabolic, and/or environmental conditions [Osuna et al. 2015]. As previously mentioned, only few genes involved in C/N balance response have been described. Our data are still far from clarifying the function of Whirly2 in this response, however the results suggest a hypothetical role of the protein during seed germination and seedlings growth, maybe by participating on response to nutrient availability.

Arabidopsis suspension cell cultures characterization

For the functional characterization of Whirly2, *Arabidopsis* suspension cell cultures were also employed. The generation of suspension cell cultures from both lines (WT and *whirly2 ko*) allowed the study at cellular level on a homogeneous population, eliminating the complexity of the presence of multiple tissue types in plants. We characterized the two cell cultures lines by analysing the fresh and dry weight (g) and the cell death percentage at different time points after

subcultures (**Figure 18 A**, **B and C**). We observed that the growth curves of the two genotypes present some interesting differences. In particular, at 2 days after subcultures the fresh and dry weight are significantly higher in *whirly2 ko* compared to WT (**Figure 18 A and B**), suggesting an increase in the mutant growth. At 8 and 9 days after subcultures, no differences in dry weight were observed between the two lines. However, *whirly2 ko* shows a significant lower fresh weight compared to WT (**Figure 18 A**), indicating a dysfunction in cell expansion. Minor differences were observed in the death percentage between *whirly2 ko* and WT cells (**Figure 18 C**). Moreover, in agreement with the results obtained in seedlings, even in cells *WHIRLY2* gene is mostly expressed in the early days after subcultures (**Figure 18 D**).

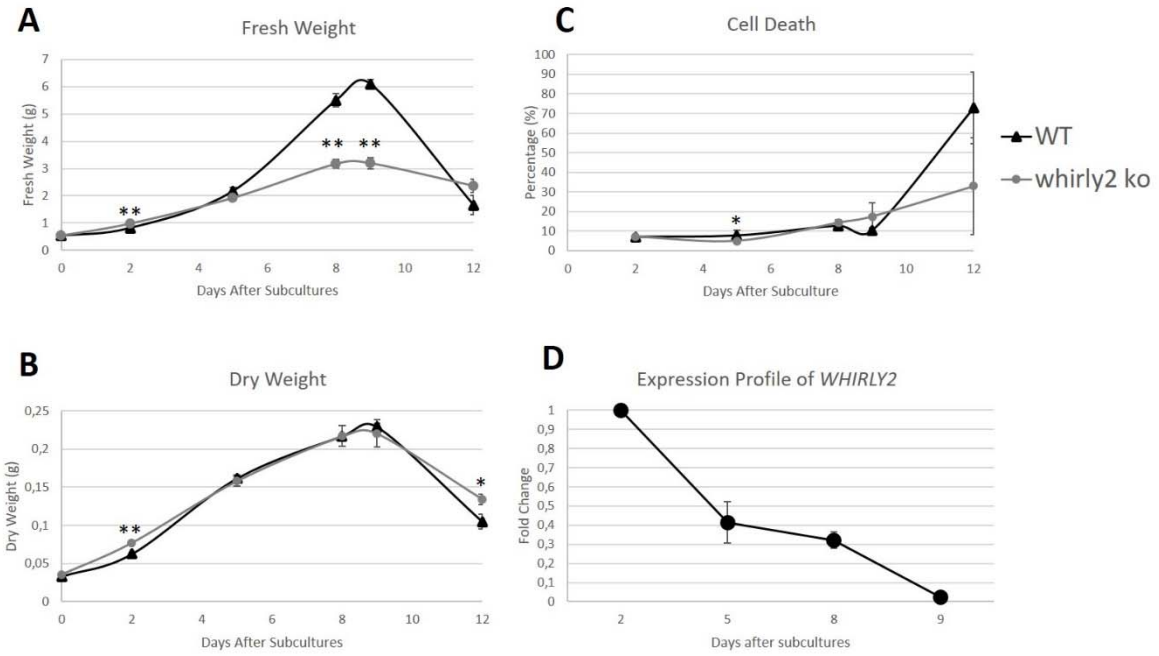

Figure 18: *WT and whirly2 ko Arabidopsis suspension cell cultures growth curves.* ***(A)*** *Fresh weight (g) at different days after subcultures.* ***(B)*** *Dry weight (g) at different days after subcultures. Samples were dried for 24 hours into a stove at 40°C.* ***(C)*** *Cell death percentage (Evans blue staining).* ***(D)*** *WHIRLY2 expression profile in WT suspension cell cultures at different days after subcultures. Values represent the mean ± standard deviation of three independent experiments performed in triplicate. The asterisks indicate values that are significantly different from WT cells using the Student's t test method (* p<0.05; ** p<0.01).*

During the development, a cell proliferation phase is accompanied or followed by a cell expansion phase. During proliferation, the organ develops by cell division, whereas during the cell expansion phase, cells do not divide anymore, but grow and differentiate [Kalve et al., 2014]. Organ growth is a tightly controlled process and a correct functioning of chloroplasts and mitochondria is necessary at any developmental stage [Van Dingenen et al. 2016]. Since Whirly2 locates in mitochondria, we can hypothesize a role of the protein in regulating cell division/expansion during the growth.

Whirly2 affects mitochondria morphology, dynamics and functionality

Since Whirly2 is targeted to mitochondria where it binds ssDNA [Cappadocia et al, 2010; Krause et al, 2005], we analysed the *in vivo* impact of the protein in this organelle. Mitochondria occupy a central role in the eukaryotic cell, including the synthesis of vitamins such as ascorbic acid, folic acid and biotin and selected amino acids; being a major site of ROS production and thus having a role in cellular signalling; as active participants in various metabolic and physiological pathways such as nitrogen assimilation, iron homeostasis and lipid metabolism; playing a central role in programmed cell death (PCD); and producing cellular energy in the form of ATP through oxidative phosphorylation.

We analysed the mitochondria morphology and dynamics in *Arabidopsis* roots and in suspension cell cultures of *whirly2 ko* and WT. Suspension cell cultures is a simple and homogeneous system compared to whole plant because cells are undifferentiated. Mitochondria were marked with tetramethylrhodamine, methyl ester (TMRM) and observed by Confocal Laser Scanning Microscope (CLSM). TMRM is a cell-permeant, cationic, red-orange fluorescent dye that is readily sequestered by active mitochondria. We observed that in roots *whirly2 ko* shows an alteration of mitochondrial morphology. While the WT mitochondria appear point-like, in *whirly2 ko* they are larger and elongated (**Figure 19**). Furthermore, in *whirly2 ko* mitochondria show a reduced motility compared to WT (data not shown). The same interesting phenotype was found in the suspension cell cultures. In *whirly2 ko* mitochondria are clearly elongated (see the inset in the figure), a morphology never observed in WT cells.

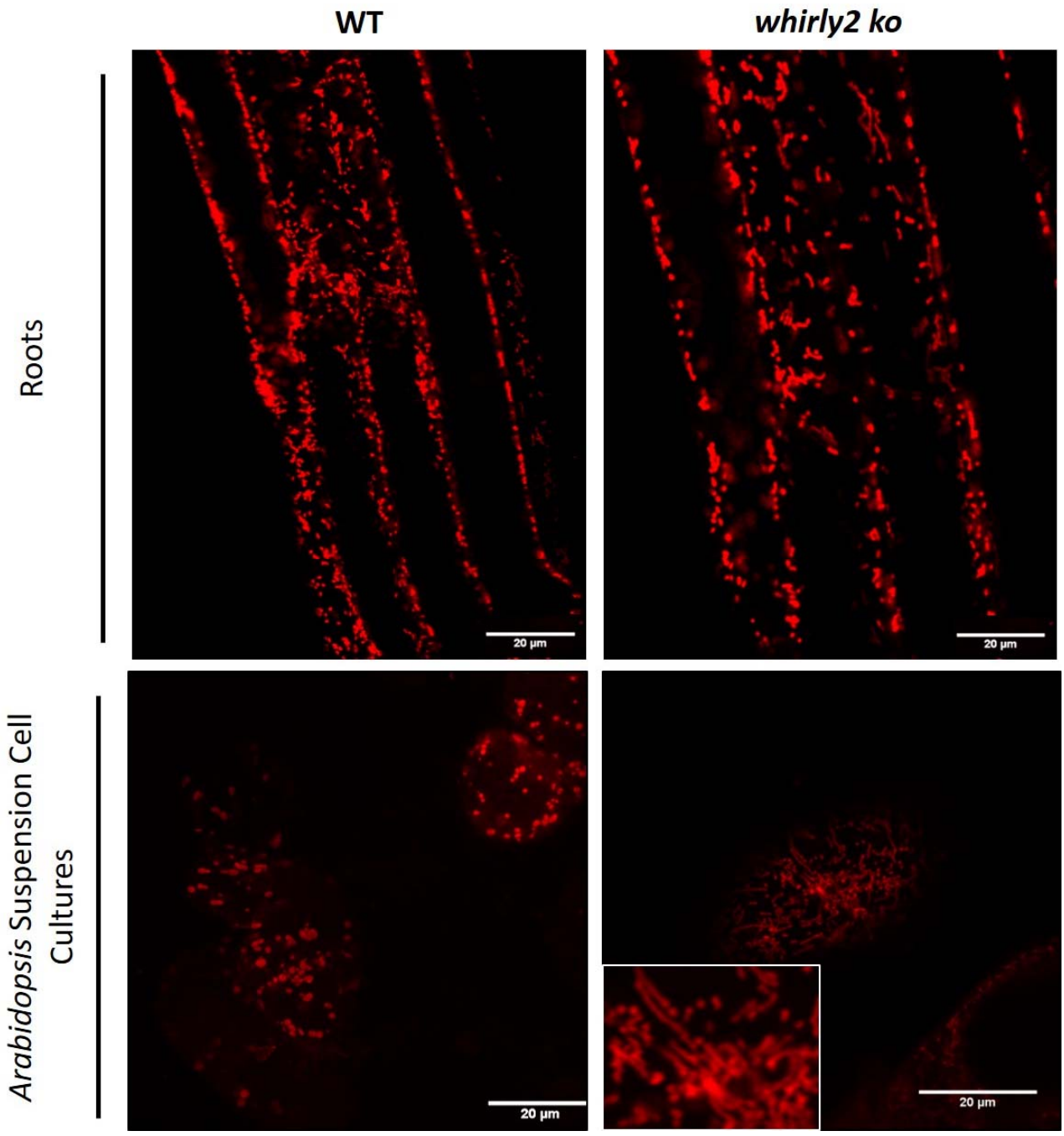

Figure 19: *Confocal Laser Scanning Microscope Images. Mitochondria are marked by 0.5 µM TMRM dye (535 nm excitation; 600 nm emission). Analyses were performed in roots and in suspension cell cultures at 5 days after sub culturing. Oil objective 63X. Inset magnification 3X.*

Mitochondria are the cell's power plant that must be in a proper functional state in order to produce the energy necessary for basic cellular functions, such as proliferation. Mitochondria are 'dynamic' in that they are constantly undergoing fission and fusion to remain in a functional state throughout the cell cycle, as well as during other vital processes such as energy supply, cellular respiration and programmed cell death. The mitochondrial fission/fusion machinery is involved in generating young mitochondria, while eliminating old, damaged and no repairable ones. As a

result, the organelles change in shape, size and number throughout the cell cycle [Horbay and Bilyy, 2016]. Our results suggest the importance of Whirly2 in maintaining a proper morphology and dynamics in plant mitochondria. Changes on mitochondria morphology and dynamics can alter the functionality of these organelles. Therefore, we analysed if the functionality of mitochondrial electron transport chain is altered in *whirly2 ko*. We evaluated oxygen consumption, alternative oxidase contribution and rotenone sensitivity in *Arabidopsis* suspension cell cultures at 5 days after subcultures. We observed that the total respiration of *whirly2 ko* cells is lower than WT, with a reduction of 10% (**Figure 20 A**). On the other hand, by adding the KCN, a complex IV inhibitor, *whirly2 ko* shows a higher capacity of alternative oxidase pathway compared to WT (**Figure 20 B**). The maximum possible flux of electrons to AOX is termed AOX capacity. Estimation of AOX capacity is analogous to estimation of an enzyme's maximum activity. The capacity is generally defined as the O_2 uptake resistant to the cytochrome pathway inhibitor and sensitive to the AOX inhibitor. This capacity measure is typically reflective of AOX protein abundance [Vanlerberghe, 2013]. Specific AOX gene family members are strongly induced at the transcript and protein level by complex III or complex IV dysfunction, suggesting that AOX expression is highly responsive to insufficient cyt pathway capacity downstream of the ubiquinone pool. However, AOX is also commonly induced by complex I dysfunction and by other disruptions in respiratory metabolism. Therefore, we treated suspension cell cultures with rotenone, an inhibitor of the complex I activity. Interestingly, we observed that in *whirly2 ko* the complex I-dependent respiration is 50% lower than in WT cells (**Figure 20 C**), suggesting a dysfunction of complex I and thus a higher contribution of alternative pathways in the mutant. To confirm this, we observed that in *whirly2 ko* cells the expression level of the *AOX* gene is higher than in WT (**Figure 20 D**), leading to a high AOX capacity, as previously described. In eukaryotes, most complex I subunits are encoded by the nuclear genome, but five to nine sub- units are encoded by mitochondrial genes. In *Arabidopsis,* various complex I mutants have been identified. Mutants with no complex I activity exhibit strongly impaired growth. A process critical to these mutants is the establishment of a seedling, which corresponds to the transition between growth fuelled by the reserves stored in the endosperm and autotrophic growth. This process requires a high amounts of energy, provided through the degradation of stored reserves. Severe complex I mutants are thus likely to be impaired in the storage of the reserves. Therefore, seed maturation is incomplete in these mutants, leading to the production of seeds with reduced reserves and viability. Another observation suggesting lower seed quality is the high variability observed

between individuals of the severe mutant lines [Vanlerberghe, 2013]. These data are in agree with the phenotype observed in *whirly2 ko*, suggesting a role of Whirly2 in contributing of complex I activity.

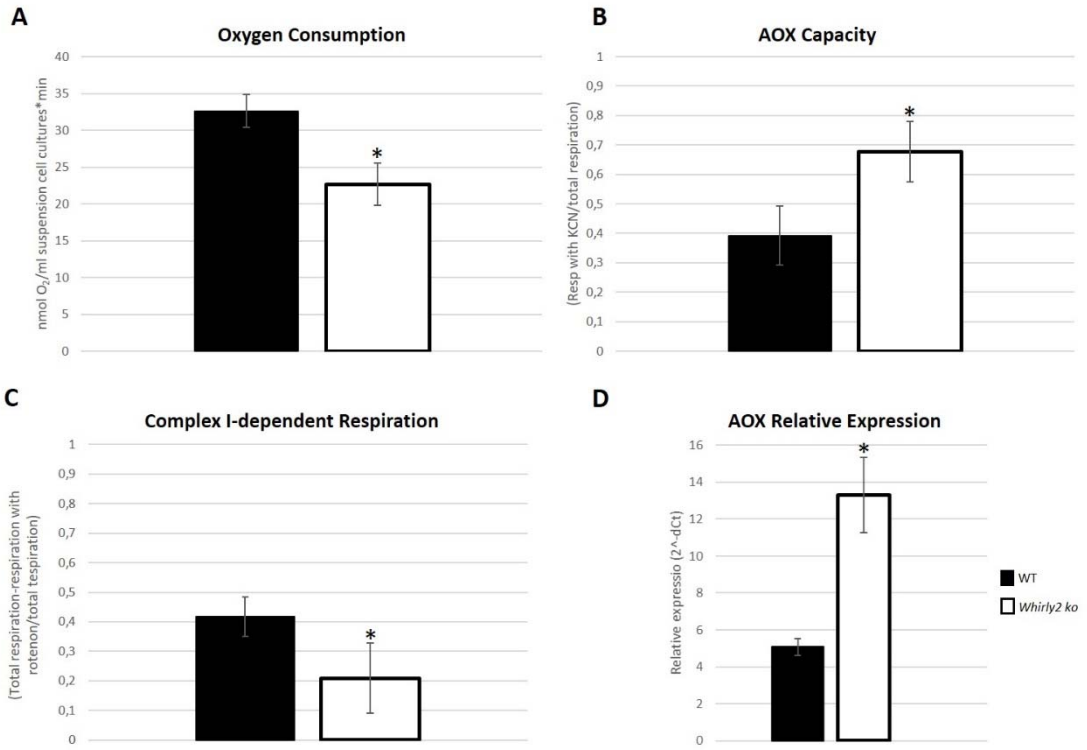

Figure 20: *Respiration analyses in WT and whirly2 ko suspension cell cultures.* ***(A)*** *Oxygen consumption without inhibitors in WT and whirly2 ko suspension cell cultures at 5 days after subcultures.* ***(B)*** *Alternative oxidase capacity. Cells were treated with KCN which is the inhibitor of complex IV.* ***(C)*** *Complex I-dependent respiration. Cells were treated with rotenone that inhibits complex I.* ***(D)*** *Relative Expression profile of the Alternative Oxidase gene in suspension cell cultures at 5 days after subcultures. The experiment was performed in control conditions of gowth. Data were normalised on actin and analyzed using the ΔCT method. Values represent the mean ± confidence interval ($p<0.05$) of three independent experiments performed in triplicate. The asterisks indicate values that are significantly different using the Student's t test method.*

Whirly2 controls nucleoids structures and regulates the amount of mtDNA and ptDNA in actively dividing cells

More detailed analysis of mitochondrial structure was performed by Transmission Electron Microscope (TEM). We analysed mitochondrial ultrastructure of *Arabidopsis* suspension cell cultures and leaves. In *whirly2 ko* mitochondria appear swollen, less electron dense compared to WT and the cristae are disorganized (**Figure 21**). Interestingly, *whirly2 ko* mitochondria show a large lucent area in which the filamentous structures of mtDNA were detected (**Figure 21**). This interesting observation reveals a disorganization of mitochondrial nucleoids, more visible in suspension cell cultures compared to somatic cells of leaves. Nucleoids are structures in which organellar DNA copies are organized in protein complexes. Together, our results suggest how the

DNA-binding protein Whirly2 plays a key role in nucleoids structure maintenance in addition to preserve the mitochondria morphology.

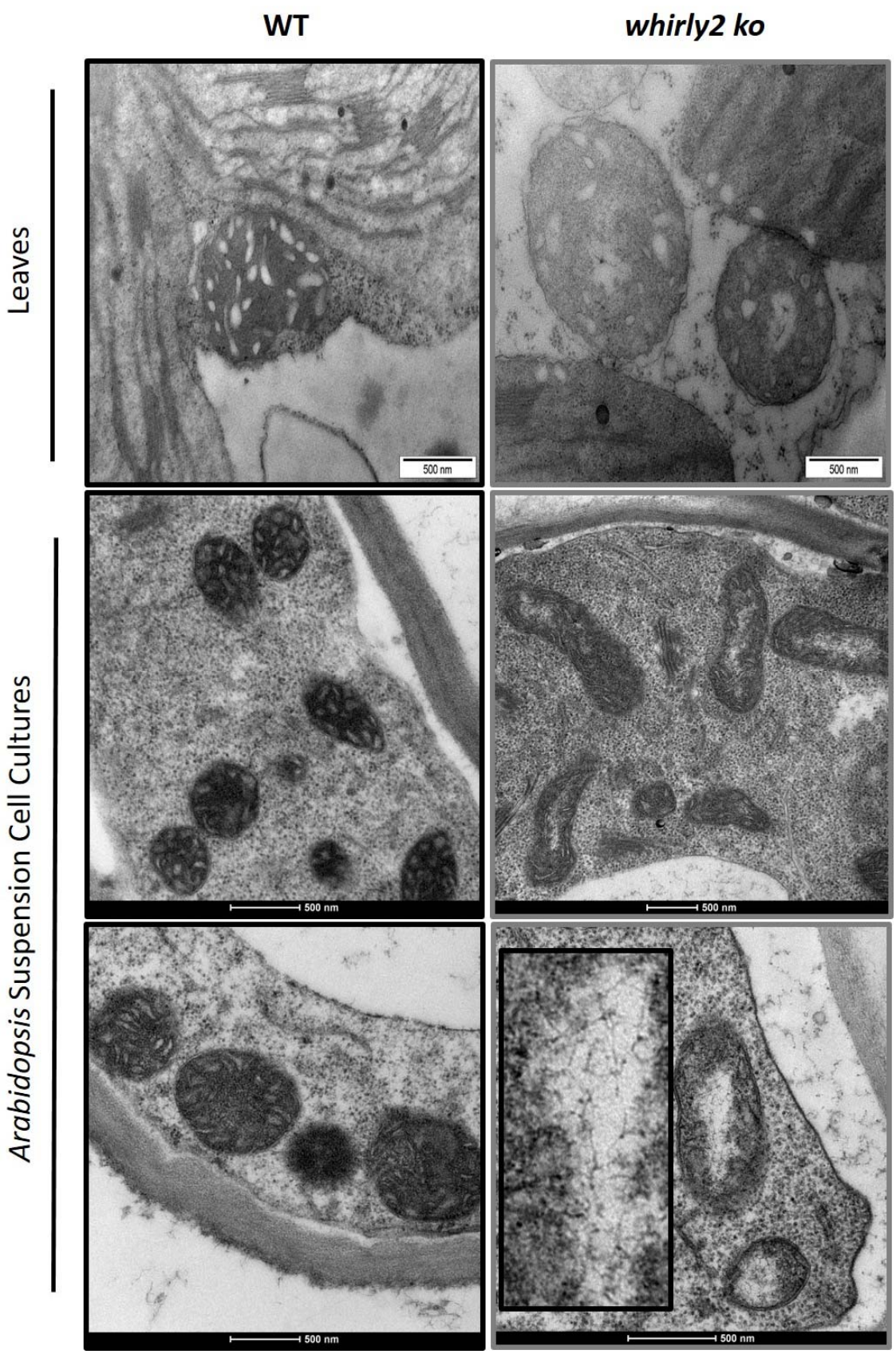

Figure 21: *Transmission electron microscope images of mitochondria from Arabidopsis leaves and suspension cell cultures at 5 days after subcultures. Whirly2 ko show alterations on morphology, cristae organisation and nucleoids structures. Inset magnification 3X.*

Whirly family was identified as proteins that bind the ssDNA and performed numerous activities related to DNA metabolism [Cappadocia et al 2010]. Among these, Whirly1 was found to bind the ptDNA in an unspecific manner and it is the major organizer of chloroplast nucleoids [Krupinska et al 2014]. Results obtained by electron microscope (**Figure 21**) demonstrate that Whirly2 plays a key role as mitochondria nucleoid organizer. Structural analysis also indicated that AtWhirly2 binding may stabilize mtDNA to favor accurate repair of DNA double-strand breaks [Cappadocia et al, 2010]. Another purpose of our study was to test whether Whirly2 could affect the copy number of mtDNA. The quantification of mtDNA was performed in *Arabidopsis* suspension cell cultures during exponential phase of growth and in 1.04 seedlings. For quantitative real-time PCR analyses, we chose the mitochondrial gene *atp1* as target and the nuclear-encoded *RpoTp* as internal standard [Preuten et al 2010]. Interestingly, in suspension cell cultures, the lack of Whirly2 significantly affects the amount of mtDNA, with a reduction of 42,8% compared to WT (**Figure 22 A**). On the other hand, no significant differences were detected in shoots and roots (**Figure 22 B**). Cai et al. 2015 found that the expression of *WHIRLY2* gene on pollen vegetative cell resulted in a 10-fold increase in mtDNA copy number. Conversely, Marechal et al. 2008 did not observed any differences in the amount of mtDNA between WT and *whirly2 ko* 4-weeks old plants. Together these data appear contradictory and probably this depends on the samples analyzed. Indeed, the mitochondria copy number differs among different organs and changes during *Arabidopsis* leaf development. Root tips contains considerably more mitochondrial gene copies per cell than all other organs. Preuten et al 2010 propose that this higher number of mitochondrial gene copies in root tips is due to large amounts of DNA in the mitochondria of dividing cells. The high amount of mtDNA in dividing cells might be a prerequisite for delivery of complete chondromes to the daughter cells/daughter generations. Probably for this reason, *Arabidopsis* suspension cell cultures on exponential growth phase contain higher amount of gene copies compared to somatic cells of shoot and root (**Figure 22**). Moreover, suspension cell culture is a homogeneous system, in which we can clearly appreciate the difference between WT and *whirly2 ko*. Conversely, the complexity and heterogeneity of the different tissue of the whole plant, can mask differences on mitochondrial copy number. These results suggest the role of Whirly2 in regulating the amount of mtDNA in actively dividing cells.

Due to the key role of organelles in cellular homeostasis, also the plastidial DNA copy number was quantified. For ptDNA quantification, we employed the *psbC* gene as target and the nuclear-encoded *RpoTp* as internal standard [Krumar Bendich 2011; Preuten et al 2010]. Interestingly, in

suspension cell cultures, the ptDNA copy number of *whirly2 ko* is lower than in WT. In particular, in *whirly2 ko* the plastidial gene copies number is reduced of 53,6% than WT (**Figure 22 A**). Conversely, no differences were observed in plant shoot and roots (**Figure 22 B**). These results suggest that Whirly2 is important not only for the regulation of mitochondrial DNA amount but also for plastidial DNA. Although it is not clear whether its effect is directed or indirect, we tried to clarify this interesting observation.

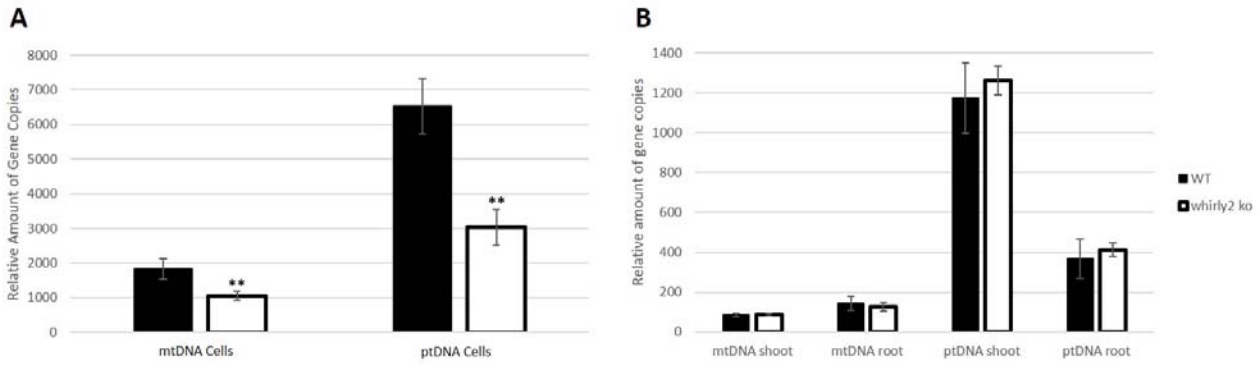

Figure 22: *Quantification of mtDNA and ptDNA in different samples.* ***(A)*** *Quantification in Arabidopsis suspension cell cultures at 5 days after subculture.* ***(B)*** *Quantification in plants at 1.04 growth stage (shoot and root). Data were analyzed using the ΔCT method. The nuclear-encoded RpoTp gene was employed as internal standard. Values represent the mean ± confidence interval ($p<0.05$) of three independent experiments performed in triplicate. The asterisks indicate values that are significantly different using the Student's t test method (** $p<0.01$).*

Plant organelle genomes are complex and the mechanisms for their replication and maintenance remain unclear. *Arabidopsis thaliana* has two DNA polymerase genes, DNA polymerase IA (PolIA) and DNA polymerase IB (PolIB), that are dual targeted to mitochondria and chloroplasts and are differentially expressed in primary plant tissues. PolIB gene expression occurs at higher levels in tissues not primary for photosynthesis. *Arabidopsis* T-DNA PolIB mutants show a 30% reduction in relative mtDNA levels, but also exhibit a 70% increase in polIA gene expression [Cupp and Nielsen, 2013]. A reduction in both mitochondrial and plastid relative genome abundance in young seedlings occurs when either of these genes is knocked out [Parent et al. 2011]. Since Whirly2 regulates the amount of organellar DNA, we investigated its impact on PolIA and PolIB. Interestingly, *whirly2 ko* cells show higher transcripts level of PolIA and PolIB than to WT (**Figure 23**). We suggest that in *whirly2 ko* the lower amount of organellar DNA induces the transcription of PolIA and PolIB. We can hypothesize that a synergistic interaction exists between Whirly2 and PolIA and PolIB functions.

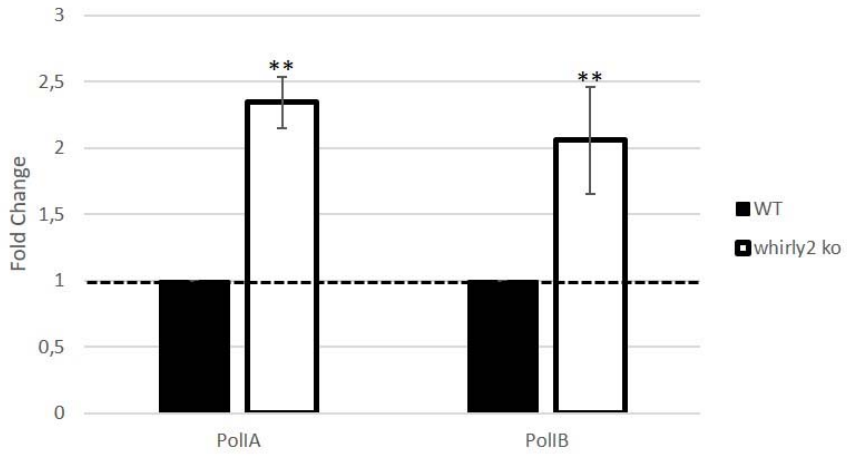

Figure 23: *Expression profile of PolIA and PolIB in suspension cell cultures at 5 days after subculture. Data were analyzed using the ΔΔCT method (WT=1). Values represent the mean ± confidence interval (p<0.05) of three independent experiments performed in triplicate. The asterisks indicate values that are significantly different using the Student's t test method (** p<0.01).*

Expression profile of *WHIRLY* genes

The effect of Whirly2 on chloroplasts lead us to hypothesize a link with the other two *WHIRLY* genes of the family. Thus, we analysed the expression pattern of *WHIRLY* genes in *whirly2 ko* and in WT plants. Mitochondria and chloroplasts play a vital role in the life of plants as they are energy producers organelles. Plants use photosynthesis to assimilate carbon and fuel their metabolism and growth. During the night, when photosynthesis is not possible, plants must rely on stored reserves of carbohydrates built up during the previous day [Scialdone and Howard, 2015]. To investigate whether the role of Whirly proteins is linked to light/dark cycle, *WHIRLY* genes expression profile at different time-points were analyzed. Gene expression analyses were performed in *Arabidopsis* seedlings at 1.04 stage grown on long day conditions (16h light/8h dark). It was observed that the expression of *WHIRLY1* and *WHIRLY3* gradually increase in the light, with a peak in the day/night transition (**Figure 24**). On the other hand, the expression of *WHIRLY2* is very low in the light period, but its expression abundantly increases in the dark (**Figure 24**). This experiment suggests that the expression profile of *WHIRLY* genes is regulated by the light/dark cycle. Moreover, the result shows the importance of Whirly2 in the dark, when the production of ATP by mitochondria becomes indispensable for plants life. In addition, the fact that *WHIRLY* genes have an opposite expression trend, suggest a possible coordination among *WHIRLY* family components.

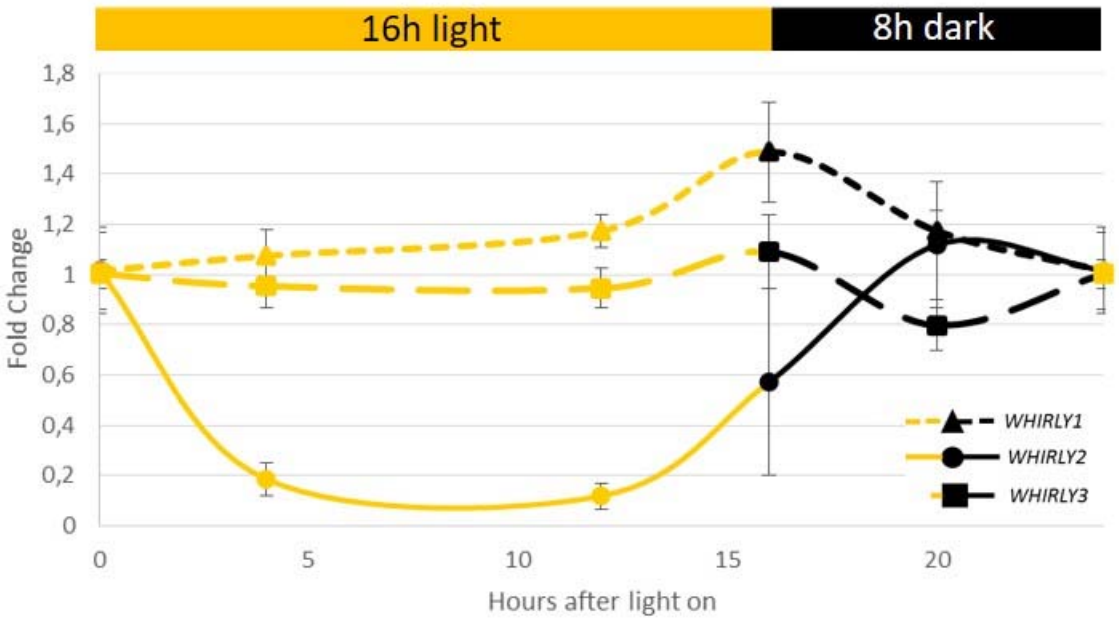

Figure 24: *Expression profile of WHIRLY genes during the light/dark cycle. The analyses were performed in 1.04 Arabidopsis seedlings growth in a long day condition. Data were normalized on point 0 (=1) and analyzed using the ΔΔCT method. Values represent the mean ± confidence interval (p<0.05) of three independent experiments performed in triplicate.*

To investigate if a coordination among *WHIRLY* genes exist, we analysed their expression profile in WT and in *whirly2 ko* plants at different developmental stages. Plants were growth under long day condition and samples were collected in the dark, when the expression of *WHIRLY2* is higher. As previously reported (**Figure 12**), *WHIRLY* genes are modulated during life cycle, with a maximum of expression in the 1.02 stage. Interestingly, the lack of Whirly2 alters the expression pattern of the others *WHIRLY* genes, particularly in the earlier stages of growth (**Figure 25**). These results suggest a coordination between *WHIRLY* genes expression during the plant growth. An intriguing feature of our results is that a mitochondrial protein can modulate the expression of genes encoding for plastid-targeted proteins. We hypothesized that the alteration of the mitochondrial functionality leads to a metabolic compensation by the chloroplast.

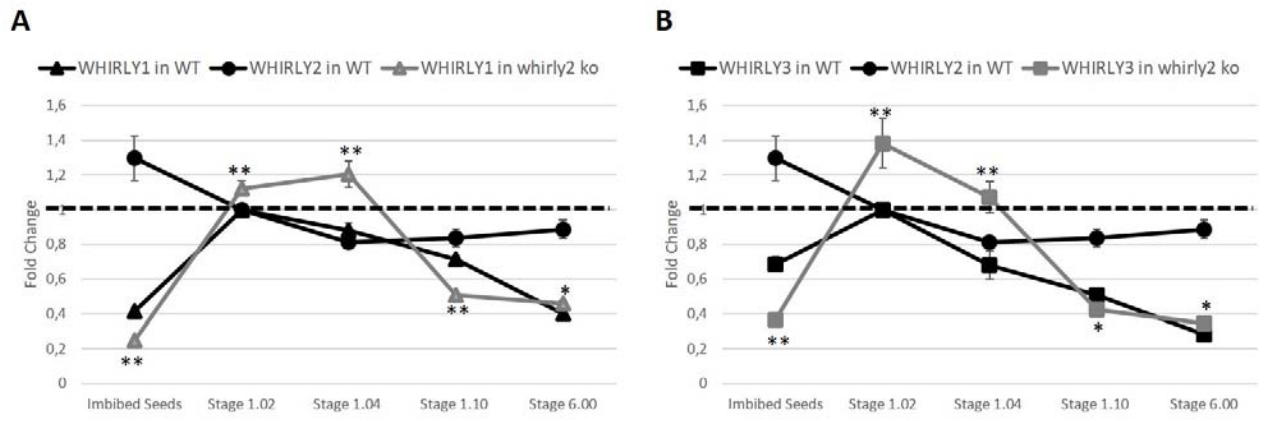

Figure 25: *Expression profile of WHIRLY genes in WT and whirly2 ko. The expression was analysed in 24 hours imbibed seeds and in plants at 1.02, 1.04, 1.10 and 6.00 stages of growth. The expression was measured in the entire plant (shoot and root) growth on MS-1/2 1% sucrose medium at long day conditions. Data were analyzed using the ΔΔCT method (WT 1.02 seedlings expression=1). Values represent the mean ± confidence interval (p<0.05) of three independent experiments performed in triplicate. The asterisks indicate values that are significantly different using the Student's t test method (*p<0.05; ** p<0.01).*

To better investigate about the modulation of gene expression mediated by Whirly2 we analysed the expression level of some nuclear-encoded genes that codify for proteins known to be involved in retrograde signalling: ANAC013 and AOX for mitochondria and CAB1 and RBCS for chloroplast. AOX is induced by various treatments with chemical inhibitors and mutations that disrupt mitochondrial function at the respiratory chain level. Therefore, AOX is used as a marker for the mitochondria retrograde regulation response in plants and ALTERNATIVE OXIDASE1a (AOX1a) is used specifically in *Arabidopsis.* AOX1a function is best studied with respect to mitochondria-initiated oxidative stress responses but is not limited to mitochondrial stress responses as evidenced by its importance in chloroplast protection during high-light stress [De Clercq et al 2013]. ANAC013 is strongly regulated by mitochondria retrograde regulation at the transcript level, and its transcript profile highly resembles the expression characteristics of the mitochondria dysfunction stimulon genes under mitochondrial perturbation as well as under environmental stress conditions [De Clercq et al 2013]. On the other hand, CAB1 (*LIGHT-HARVESTING COMPLEX B*, coding for chlorophyll binding protein) and RBCS (Rubisco) are nuclear-encoded, plastid-localized proteins which are regulated under chloroplast stress conditions. In particular, the nuclear genes *cab1* and *RbcS* were repressed when the plastids were dysfunctional after photo-oxidation [Pfannschmidt 2010]. Interestingly, *whirly2 ko* show a higher transcript level of these four genes under control conditions of growth (**Figure 26**).

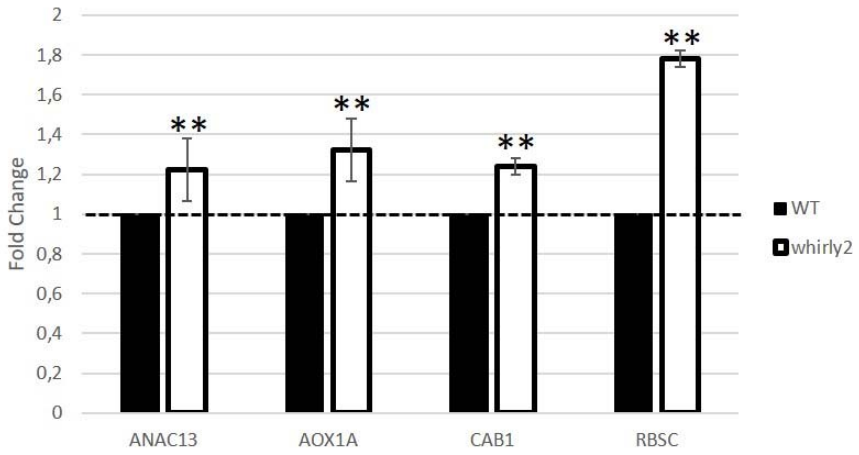

Figure 26: *Expression profile of target genes of organellar signals in seedlings at 1.04 stage of growth. The expression was measured in the whole plant (shoot and root) growth on MS 1,5% sucrose medium at long day conditions. Data were analyzed using the ΔΔCT method (WT seedlings expression=1). Values represent the mean ± confidence interval ($p<0.05$) of three independent experiments performed in triplicate. The asterisks indicate values that are significantly different using the Student's t test method (**$p<0.01$).*

Since the expression patterns of genes are altered in *whirly2 ko* we analysed the response of the mutant at different stressors. Plants were growth in medium with 50 µM of antimycin or 50 mg/L of spectinomycin. Antimycin is an inhibitor of complex III of the mitochondria respiratory chain, while spectinomycin blocks the chloroplasts development (**Figure 27 A**). When WT plants are grown on antimycin and spectinomycin, *WHIRLY* genes are up regulated compared to control condition (**Figure 27 B**). Interestingly, *WHIRLY2* is highly induced by spectinomycin, indicating a key role of the protein when chloroplasts are not functional, a situation in which energy production by mitochondria is essential. As reported previously, Whirly2 has an important role on germination and on early stages of growth before chloroplasts development. Together, these results suggest a role of Whirly2 in developmental or stress situations that required an enhanced energy production by mitochondria. Moreover, we observed that in *whirly2 ko* antimycin is unable to induce the expression of *WHIRLY1* and *WHIRLY3* like in WT (**Figure 27 B**), confirming that Whirly2 is involved in the regulation of the expression of the other *WHIRLY* genes. In addition, we observed that also the expression pattern of genes that codify for proteins know to be involved in retrograde signalling is modified in *whirly2 ko* under stress conditions (**Figure 27 C and D**). Although these data are preliminary, they suggest the importance of the Whirly2 protein in coordinating plant organelles communication in developmental and stress responses, in particular when an enhanced energy production by mitochondria is required.

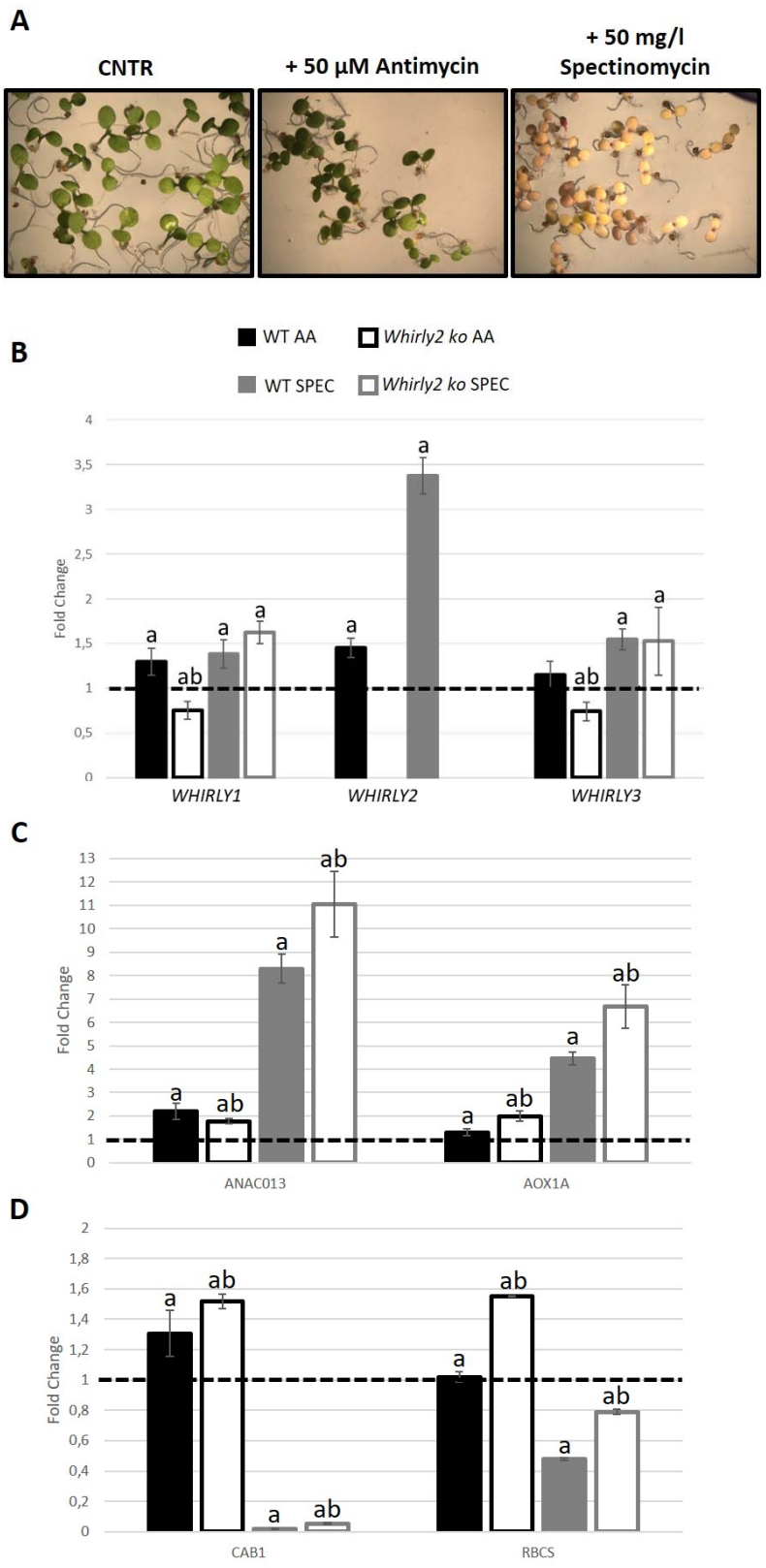

Figure 27: *Expression profile of target genes of organellar signals in the whole seedling (shoot and root).* ***(A)*** *Arabidopsis seedlings were growth till stage 1.04 on control media (MS 1,5% Sucrose), medium with 50 µM of antimycin or 50 mg/L of spectinomycin.* ***(B)*** *WHIRLY genes expression.* ***(C)*** *Expression of target genes of mitochondrial signals.* ***(D)*** *Expression of target genes of chloroplastic signals. Data were analyzed using the ΔΔCT method (WT CNTR expression=1). Values represent the mean ± confidence interval (p<0.05) of three independent experiments performed in triplicate. (a=significant different from WT CNTR; b= significant different from WT treated). The significance was calculated using the Student's test method.*

CONCLUSIONS

Organisms perceive and respond to developmental and environmental cues through tightly regulated inter- and intracellular communication networks. The integrity of this communication circuitry enables cellular homeostasis sustained through interorganellar interactions that are controlled by processes known as anterograde (nucleus to organelle) and retrograde signaling (organelle to nucleus) [de Souza et al 2017]. Mitochondrial retrograde signals have not been well studied in plants, in contrast to those in chloroplasts. Recently, among the putative molecules involved in the retrograde signalling between chloroplast and nucleus, it was identified the Whirly1 protein. Whirly1 belongs to a small plant-protein family that also includes Whirly3, located into chloroplasts, and Whirly2 with a mitochondrial localization. The aim of this PhD project was to elucidate the *in vivo* role of the mitochondrial protein Whirly2 in order to evaluate a possible involvement in the retrograde signalling from mitochondria and nucleus. Our study suggests that the protein plays a relevant role in seed development and germination. During these stages, plants are heterotrophic and the growth completely depends on the reserves stored in the seed and by their mobilization. These processes require a high amount of energy that mostly derives from mitochondrial activity. We observed that the phenotype of *whirly2 ko* is associated with an alteration of mitochondria morphology, dynamics and cristae organization. Consequently, also the functionality of the organelle is modified, particularly we observed an alteration of mitochondria respiration. *Whirly2 ko* suspension cell cultures show a higher alternative oxidase contribution and a lower complex-I dependent respiration compared to WT. The alteration at mitochondria level is associated to the fact that Whirly2 is a nucleoid protein. By the way, in *whirly2 ko* cells we observed an alteration of the mtDNA copy number content. It is hypothesized that nucleoid proteins act as scaffolds for the proteins involved in mitochondrial morphology and dynamic regulation. In the mutant, we noted a clear phenotype at seed level but not in the adult organisms. Probably, in plants chloroplasts can metabolically compensate the deficiency of energy provided by mitochondria, while in the embryo chloroplasts are not yet developed. In support of this hypothesis we observed that in plants, but not in the seed, the expression of *WHIRLY1* and *WHIRLY3* genes is induced. Since Whirly proteins alter the ptDNA level, the induction of their expression can influence the functionality of chloroplasts. Furthermore, proteins with organelles

localization, are involved in informing the nucleus about the state of the cell. Interestingly, we also observed that alterations in chloroplasts strongly induce the transcription of *WHIRLY2* gene, confirming a compensatory mechanism between *WHIRLY* genes. Our data provide new information about the role of the mitochondrial protein Whirly2 in plant cells. All together, our results suggest an intriguing involvement of Whirly proteins in the integration of cellular signals to maintain the homeostasis of the cell.

PUBLICATIONS

Storti M, Costa A, Golin S, Zottini M, Morosinotto T, Alboresi A. Long-distance calcium waves are an early adaptation event during plant land colonization. Accepted by *Plant and Cell Physiology*.

D'Alessandro S, Golin S, Hardtke CS, Lo Schiavo F, Zottini M (2015). The co-chaperone p23 controls root development through the modulation of auxin distribution in the Arabidopsis root meristem. *Journal of Experimental Botany* 66(16): 5113-5122.

Journal of Experimental Botany, Vol. 66, No. 16 pp. 5113–5122, 2015
doi:10.1093/jxb/erv330 Advance Access publication 10 July 2015
This paper is available online free of all access charges (see http://jxb.oxfordjournals.org/open_access.html for further details)

RESEARCH PAPER

The co-chaperone p23 controls root development through the modulation of auxin distribution in the *Arabidopsis* root meristem

Stefano D'Alessandro[1], Serena Golin[1], Christian S. Hardtke[2], Fiorella Lo Schiavo[1], and Michela Zottini[1]

[1] Department of Biology, University of Padova, Via U. Bassi 58/B, I-35131 Padova, Italy
[2] University of Lausanne - Biophore Building, DBMV CH-1015 Lausanne, Switzerland

To whom correspondence should be addressed. E-mail: michela.zottini@unipd.it

Received 11 May 2015; Revised 11 June 2015; Accepted 12 June 2015

Editor: Angus Murphy

Abstract

Homologues of the p23 co-chaperone of HSP90 are present in all eukaryotes, suggesting conserved functions for this protein throughout evolution. Although p23 has been extensively studied in animal systems, little is known about its function in plants. In the present study, the functional characterization of the two isoforms of p23 in *Arabidopsis thaliana* is reported, suggesting a key role of p23 in the regulation of root development. *Arabidopsis* p23 mutants, for either form, show a short root length phenotype with a reduced meristem length. In the root meristem a low auxin level associated with a smaller auxin gradient was observed. A decrease in the expression levels of PIN FORMED PROTEIN (PIN)1, PIN3, and PIN7, contextually to an inefficient polar localization of PIN1, was detected. Collectively these results suggest that both *Arabidopsis* p23 isoforms are required for root growth, in particular in the maintenance of the root meristem, where the proteins are located.

Key words: *Arabidopsis*, auxin, p23-chaperone, pin formed protein (PIN), polar auxin transport, root growth.

Introduction

Root growth and development are fundamental processes for the life of plants, controlling water uptake, nutrient acquisition, anchorage to soil, and secondary metabolite synthesis and storage (Saini *et al.*, 2013). Post-embryonic growth and development are controlled through the meristems, which generate differentiating cells that shape adult plant structures (Moubayidin *et al.*, 2009). Meristem maintenance is controlled through a finely regulated orchestration of hormones and signalling molecules, among which auxins are indeed the master regulators of root development (Saini *et al.*, 2013). Auxin is virtually involved in all phases of plant growth and development, and auxin signalling is regulated at the level of biosynthesis, transport, and perception (Saini *et al.*, 2013). From the sites of biosynthesis (Ljung *et al.*, 2005), auxin is actively transported via the combination of two routes involving the long-distance transport through mature phloem and cell-to-cell polar transport (PAT), mediated through specific influx/efflux carriers (Vieten *et al.*, 2007; Geisler *et al.*, 2014). AUX1 and LAX (LIKE-AUX1) are major auxin importers, whereas PIN (PIN FORMED PROTEIN) and ABCB (ATP-BINDING CASSETTE B) are the main families of auxin exporters (Geisler and Murphy, 2006; Verrier *et al.*, 2008; Krecek *et al.*, 2009). At the site of action, auxin perception is mediated through members of the TIR1 (TRANSPORT

INHIBITOR RESPONSE 1)/AFB family. TIR1 is an F-box subunit of the ubiquitin ligase complex SCF^{TIR1}, which interacts with and ubiquitinates Aux/IAA proteins (AUXIN/INDOLE-3-ACETIC ACID) (Gray *et al*., 2001). Aux/IAA proteins are auxin response inhibitors that interact and block ARF (AUXIN RESPONSE FACTOR) transcription factors (Mockaitis and Estelle, 2008). Indole-3-acetic acid (IAA) is the most abundant natural auxin, and the apoplastic acidic environment facilitates the protonation of IAA to IAAH, which diffuses into cells. Due to the chemical nature of auxins, PIN and ABCB exporters are the primary control elements of PAT (Geisler and Murphy, 2006). Auxin signalling continuously crosses pathways with other hormones and signalling molecules in a complex chain of feedback controls (Dello Ioio *et al*., 2008; Overvoorde *et al*., 2010; Saini *et al*., 2013). In particular, auxins and cytokinins are the major players of a well-known crosstalk mechanism that regulates root meristem maintenance and consequent root growth (Moubayidin *et al*., 2009). Cytokinin–auxin crosstalk occurs at the transport level of auxin signalling through a regulatory circuit converging on the type-B ARR1 (ARABIDOPSIS RESPONSE REGULATOR 1) transcription factor and consequently on the SHY2 (SHORT HYPOCHOTHYL 2) protein, which negatively regulates the expression of PIN genes (Dello Ioio *et al*., 2008).

The small acidic protein, p23, has been identified in animal systems as an HSP90 co-chaperone (Johnson and Toft, 1994), which stabilizes the active conformation of the progesterone-receptor HSP90 complex after binding to the ATP-bound form of HSP90 and lowering the ATPase activity rate of HSP90 (Chadli *et al*., 2000; Ali *et al*., 2006; Li *et al*., 2012). Two homologues of p23 have been identified in *Arabidopsis*: p23-1 (At4g02450) is 241 amino acids in length with a mass of 25.47 kDa, whereas p23-2 (At3g03773) is 150 amino acids in length with a mass of 17.4 kDa (Zhang *et al*., 2010). Each isoform shares 27% and 25% amino acid identities with human p23, respectively, and shows 38–60% identity with other plant p23 homologues. The difference in length of p23-1 and p23-2 reflects a glycine rich (MG/GA) segment of 70 amino acids in the C-terminal region of p23-1, whose function is not yet understood. Both plant p23 isoforms and the chimeric protein p23-1-d (lacking the glycine rich tail) bind to HSP90 *in vitro*; however, unlike their animal counterpart, these proteins do not reduce the chaperone ATPase activity rate (Zhang *et al*., 2010).

Although *Arabidopsis* p23 isoforms have been the object of previous biochemical characterization studies (Zhang *et al*., 2010; Tosoni *et al*., 2011), the physiological role of these proteins remains elusive. These analyses revealed that p23 proteins are chiefly located in the root meristem, where they intervene in the regulation of root growth and development.

Material and methods

Plant materials and growth conditions

All experiments were performed using *Arabidopsis thaliana* ecotype Columbia (Col-0). The mutant seedlings for *p23-1* (SAIL 245_ H06), *p23-2* (SALK_003076), and *arr1-4* (SALK_042196) were obtained from the European *Arabidopsis* Stock Centre (NASC). T-DNA insertions were verified through PCR (primers are listed in Supplementary Table S1 available at *JXB* online). From the p23 single mutants, a double mutant *p23-1*×*p23-2* (*dKO*) was generated. The plant seeds were surface sterilized in 70% EtOH and 0.05% Triton X-100, followed by 100% EtOH. The seeds were sown onto square Petri dishes containing one-half-MS medium supplemented with 0.5 g/l MES-KOH, pH 5.7, 0.8% Plant Agar (Duchefa), and 1% Sucrose, stratified for 2 d at 4 °C in the dark, and placed vertically in a growth chamber under a long daylight period (16 h light/ 8h dark) using 150 µmol m^{-2} s^{-1} at 22 °C. The translational reporter plants, pp23-1:p23-1-GUS and pp23-2:p23-2-GUS, were generated after transforming the single mutants *p23-1* or *p23-2* with *Agrobacterium* harbouring a construct containing the entire sequence of the *p23-1* or *p23-2* genes, starting from base pair −540 or −3191, respectively, fused to the β-Glucuronidase reporter gene (*UID*-A; the primers are reported in Supplementary Table S1) and subcloned into the pGreen 0029 binary vector (Hellens *et al*., 2000). Complemented lines p23-1 T 35S:p23-1 and p23-2.1 T 35S:p23-2 were generated after trans- forming the single mutants *p23-1* or *p23-2* with *Agrobacterium* har- bouring a construct containing the coding sequence (CDS) of p23-1 or p23-2 under the control of the CaMV 35S constitutive promoter (primers for CDS cloning are reported in Supplementary Table S1) and subcloned into the pGreen 0029 binary vector (Hellens *et al*., 2000). The reporter lines DR5:GUS, DII-Venus, PIN1-GFP, PIN7- GFP, or the mutant line *arr1-4*, were crossed with the *dKO* line, and the F2 homozygous lines were used for subsequent analyses.

RNA isolation and qRT-PCR

Seven days after germination (dag), the roots and shoots of wild-type and mutant seedlings were harvested separately for subsequent analyses. Total RNA was extracted from plant samples using TRIzol® Reagent (Invitrogen) according to the manufacturer's instruc- tions. First-strand cDNA synthesis was performed using 1 µg of RNA, oligo(dT) primers, and SuperScript-II Reverse Transcriptase (Invitrogen) according to the manufacturer's instructions. The primers for qRT-PCR (quantitative real-time PCR) are shown in Supplementary Table S1. The expression levels of each gene were normalized to the expression level of the housekeeping genes *Actin-2* (ACT2; At3g18780) or *elf1a* (At5g60390), as indicated.

Root growth assay

The plant seeds from the different genotypes were sown onto solid growth medium, and vertically grown as described above. Plates were scanned using a flatbed scanner every day from the fourth to the 10th dag. The roots were analysed at different developmental stages through image analysis (Fiji – ImageJ bundle software). The experiments were performed at least three times and each sample comprised 25 seedlings.

For N-1-naphtylphtalamic acid (NPA) and auxin treatments, 5-d-old seedlings were transferred to growth medium supplemented with different concentrations of NPA, IAA, or 1-Naphthaleneacetic acid (NAA; Sigma-Aldrich). After 5 d of treatment, the primary root length was measured as described above.

β-Glucuronidase histochemical assay

Histochemical staining was performed at different developmental stages. Samples were analysed for β-glucuronidase activity. The samples were incubated for variable times (1 h to overnight) at 37 °C in the reaction medium (2 mM X-Gluc, 0.05% Triton X-100, 5 mM $K_3Fe(CN)_6$, 5 mM $K_4Fe(CN)_6$ 3× H_2O, 10 mM EDTA, and 50 mM sodium phosphate buffer, pH 7.0). The seedlings were mounted on chloral hydrate solution. The images were captured using a microscope (Leica 5000B) with Normarsky correction (DIC). The experiments were performed at least in triplicate, and each sample set comprised 10 seedlings.

Confocal microscopy

Seven-day-old seedlings were mounted in a drop of 2% (20 µg/ml) propidium iodide (PI; Sigma-Aldrich) solution, on a microscope slide, and the images were acquired using a LEICA SP5 laser scanning confocal imaging system. The excitation and emission wavelengths are reported in the image captions. High-definition images were acquired (1024 × 1024, 25× objective) and analysed using the Fiji – ImageJ bundle software (http://fiji.sc/Fiji). The experiments were performed at least in triplicate, and each sample set comprised 10 seedlings.

Statistics

All experiments were performed at least in triplicate, and the images represent typical examples. The values are represented as the means ± standard deviation. The statistical significance was demonstrated using Student's *t*-test.

Results

p23-1 *and* p23-2 *knockout mutants show shorter roots*

To investigatethefunctionalroleof p23 proteinsin *Arabidopsis*, knockout mutant lines of the two isoforms were isolated and phenotypically characterized. Although the aerial part of the plant showed no altered traits throughout the plant development, root growth was strongly impaired in single and double (*dKO*) mutants (Fig. 1A). In particular, in 10-d-old single mutant seedlings, the primary root length was approximately 70% that of the wild-type (wt) (wt=5.3±0.36 cm; *p23-1*=4.17±0.15 cm; and *p23-2*=4.31±0.15 cm) (Fig. 1B). In mutant lines, the reduction in root growth was evident and significant from the seventh dag compared with that of the wild-type (Fig. 1B). The short-root phenotype, detectable only at an advance stage of development, suggests that the p23 mutants are likely impaired in meristem maintenance rather than in the early post-embryonic stages of root growth. Double knockout mutants were generated after crossing *p23-1* and *p23-2* (*dKO*). The latter provides information for determining whether these two proteins play a role in the same pathway controlling root growth and to evaluate the contribution of each isoform to this process. The primary root length of the *dKO* line is comparable with that of both single knockout mutants (*dKO*=4.17 ± 0.2 cm), as shown in Fig. 1A and B, thus showing no additive effect of the two mutations. This behaviour suggests that although not redun- dant, the two proteins intervene in the same process regulating root growth.

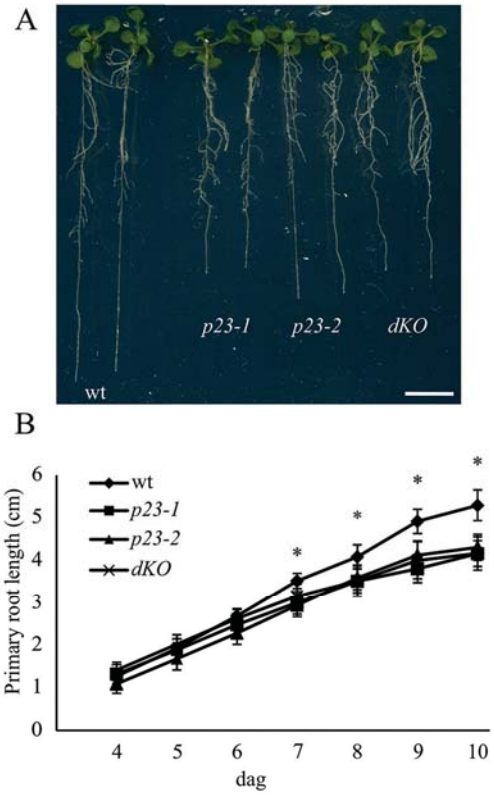

Fig. 1. p23 knockout mutants show shorter roots compared with the wild-type. (A) Twelve-day-old *Arabidopsis* seedlings of wild-type (wt), *p23- 1*, *p23-2*, and double knockout (*dKO*) background. p23 single knockout mutants and the double knockout mutant show shorter roots as compared with the wild-type. (B) Quantification of the primary root length of the different backgrounds: wt, *p23-1*, *p23-2*, and *dKO* from the fourth to the 10th dag. The short-root phenotype is characterized by a slower root growth appreciable from the seventh dag (**P*<0.01, Student's *t*-test). Scale bar = 1 cm. (A colour version of this figure is available at *JXB* online.)

Localization and expression profile of p23-1 *and* p23-2

To evaluate the expression profile of the two genes, the transcripts of *p23-1* and *p23-2* were analysed through qRT-PCR during plant development (1–5-week-old plants). As reported in Fig. 2A, both isoforms are expressed at all growth stages. *p23-1* is the most expressed isoform ranging from 20–50% of *elf1a* expression, whereas p23-2 expres- sion ranges from 2–5% of *elf1a* expression. This result demonstrates a 10-fold higher expression of the long isoform than that of the short isoform, during the first 4 weeks and suggests that p23-1, although showing a similar phenotype in the roots, is the major p23 isoform present in plants.

The expression and localization of p23-1 and p23-2 was determined at cellular level *in planta*. The short isoform p23-2 was previously described as nuclear and cytosolic (Tosoni *et al.*, 2011). To analyse the subcellular localization of the long isoform p23-1, stably transformed *Arabidopsis* plants expressing the protein under the control of the constitutive viral promoter CaMV 35S were generated. In these plants, the fusion protein p23-1, tagged at the C-terminus with YFP, was expressed in all tissues. These transgenic lines showed florescence throughout the plant body. The analysis of different plant tissues using confocal laser microscopy defined the subcellular localization of the chimeric protein. p23-1-YFP was detectable in leaves of 10-d-old seedlings (Supplementary Fig. S1 available at *JXB* online) with a cytosolic and nuclear localization and similarly in all analysed tissues.

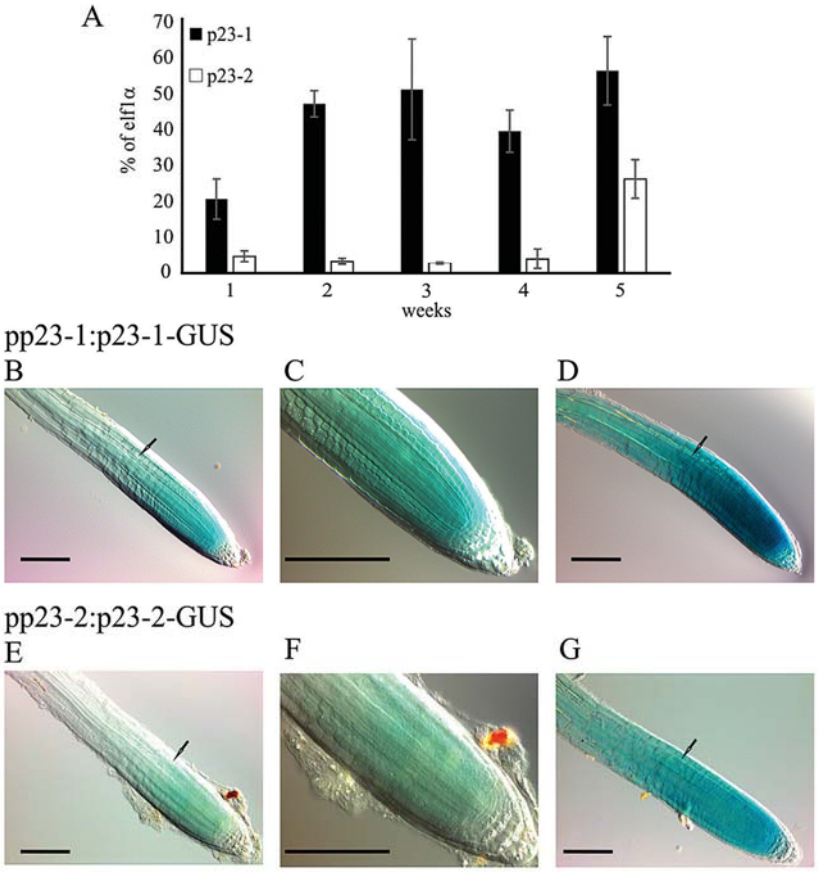

Fig. 2. Transcript levels of *p23-1* and *p23-2* and protein localization *in planta*. (A) Quantitative real-time analyses of the transcript levels of *p23-1* and *p23-2* in *Arabidopsis* plants, grown in soil from 1–5 weeks. Data are reported as percentage of *elf1α* transcript levels. (B–G) Histochemical analyses of the translational reporter of p23-1 and p23-2. (B, E) pp23-1:p23-1-GUS and pp23-2:p23-2-GUS *Arabidopsis* staining (30 min) concentrates in the root meristem and drops above the first full-elongated cell (arrow). (C, F) Magnification of the root meristem. (D, G) Four hours of GUS staining reveals that both p23 proteins appear also in the upper part of the root. Scale bar = 100 μm. (A colour version of this figure is available at *JXB* online.)

To examine the expression and localization of the two proteins in the entire plant, stable transformed *Arabidopsis* plants expressing the β-glucuronidase gene (*UID-A*) fused either to *p23-1* or *p23-2* were generated. The reporter allowed defining the localization of the two proteins through a histochemical assay. Several transgenic lines were obtained and seedlings at different developmental stages were analysed.

In 3–10-d-old seedlings, the presence of the chimeric proteins is detectable in the root meristematic zone, where they strongly concentrate (Fig. 2B, C–F). Four hours of staining let the signal appear in the vascular tissue of the roots (Fig. 2D, G) and after 16 h the reporter was detected in the entire root and in the vasculature of the leaves (data not shown). It is worthwhile to highlight that the two proteins are highly expressed in the root meristem and the signal drops at the level of the first full-elongated cell (black arrows, Fig. 2B–G). Furthermore, the difference in the expression level of the two isoforms, observed by qRT-PCR (Fig. 2A), was confirmed by the histochemical assay. In fact, although p23-1-GUS is detectable in the root meristem after 5 min of staining, p23-2-GUS shows comparable levels only after 30 min.

p23 mutants show a reduced number of dividing cells in the root meristem

The structure of the primary root was accurately analysed in wild-type and mutant lines by confocal microscopy. For this purpose, root width, meristem length, and cell number, in the zone between the quiescent centre and the first cortical elongating cell, were measured (Moubayidin *et al.*, 2013). These analyses revealed that roots of the different genotypes have a comparable width, whereas a significant difference was observed in the length of the meristematic zone (Fig. 3A). As shown in Fig. 3B, both single and *dKO* lines showed a reduced number of cortical cells in the root meristem compared with the wild-type (wt=41.8±3.2; *p23-1.1*=31±4; *p23-2.1*=26±4.8; *dKO*=30 ± 4.8). To verify the causality between the deficiency of p23 proteins and short-root phenotype, stable transformed lines overexpressing p23-1-HA or p23-2-HA were generated in

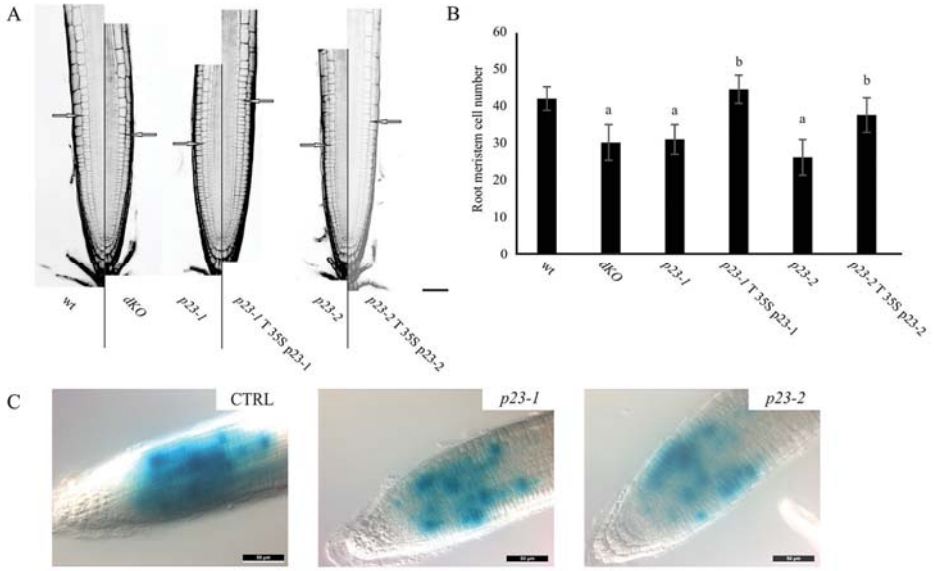

Fig. 3. p23 mutant lines show a reduced number of cells in the root meristematic zone. (A) PI stained root of 7-d-old seedlings of the different lines. Excitation and emission wavelengths for confocal acquisition are 488 nm and 600–650 nm, respectively. The arrows show the upper limit of the meristematic zone. Scale bar = 50 μm. (B) Meristem cell number in the different genetic backgrounds. p23 mutant lines show a reduced number of cortical cells in the root meristematic zone, while complemented lines show no difference as compared with the wild-type ($^{a}P<0.01$ compared with the wt, $^{b}P<0.01$ compared with the background line; both Student's *t*-test). (C) Histochemical analysis of the CyclinB1:GUS reporter in the wild-type (CTRL), *p23-1*, or *p23-2* background. Scale bar = 50 μm. (A colour version of this figure is available at *JXB* online.)

the *p23-1* (*p23-1* T p23-1-HA) or *p23-2* (*p23-2* T p23-2-HA) background, respectively. As reported in Fig. 3A and B, the overexpression of p23 proteins could complement the respective mutant lines both in terms of meristem length and cortical cell number (*p23-1* T p23-1=44.3±3.8; *p23-2* T p23-2=37.40±4.7).

To assess whether the reduction in meristem cell number could reflect the loss of meristematic-cell-division potential, the expression of *pCyclinB1:GUS* (a broadly used marker to indicate the G2-to-M phase of the cell cycle) was monitored (Colón-Carmona *et al.*, 1999) in wild-type, and *p23-1* and *p23-2* single mutants, to visualize root meristem cells in the G2–M phase. As shown in Fig. 3C, the *pCyclinB1:GUS* in both *p23-1* and *p23-2* backgrounds showed a strong reduction in the intensity and extent of GUS staining as compared with the wild-type background (CTRL). This result demonstrated that cell division is impaired in the root meristem of both the single mutant lines, further suggesting a common pathway for the two isoforms in regulating root growth.

Auxin distribution is altered in p23 mutants

A p23 double knockout mutant harbouring the DR5::GUS construct was generated to evaluate whether auxin distribution was altered. DR5 is a widely used auxin molecular marker (Ulmasov *et al.*, 1997) that allows the detection of cellular responses to auxin using a histochemical assay. As shown in Fig. 4A, strong DR5 activity was detected in the wild-type primary root (upper panel), particularly at the level of columella cells and the quiescent centre (QC), whereas lower expression was observed in *dKO* plants (lower panel).

To obtain a more detailed analysis of auxin distribution in the meristem at the cellular level, the DII-Venus auxin responsive marker line was crossed with the *dKO* line, leading to a more direct detection system for auxin in the mutant (Brunoud *et al.*, 2012). Analyses of DII-Venus fluorescence using laser scanning confocal microscopy (Fig. 4B) showed that DII-Venus fluorescence was higher in the root meristem of the *dKO* line (lower panels) than in wild-type plants (upper panels). In particular, higher levels of fluorescence were detected in the root cap, epidermis, and columella cells—tissues that are typically characterized by auxin accumulation (Krecek *et al.*, 2009). However, the fluorescent signal was not detectable at the level of the quiescent centre in both wild-type lines, as expected, and p23 mutants, suggesting that this mutation does not compromise auxin levels in the QC. Indeed, the expression of ASB1 (ANTHRANILATE SYNTHASE BETA SUBUNIT 1) and YUC6 (YUCCA 6) in the shoot of *dKO* plants was similar to that of wild-type plants, whereas slightly enhanced expression was observed in the roots (Supplementary Fig. S2 available at *JXB* online). This result suggests that alterations in auxin levels in the roots do not depend on the lower biosynthetic rate of the hormone. Furthermore, it was observed that in *dKO* mutants treated at 5 dag with 10 nM of either IAA or NAA, the wild-type primary root length was rescued (Fig. 4C, D), thus directly associating the short-root phenotype with low auxin content at the root level. These results suggest that alterations in auxin sensing can be excluded. Moreover, both IAA and NAA restored normal root growth, suggesting that the *dKO* line is not altered in auxin influx.

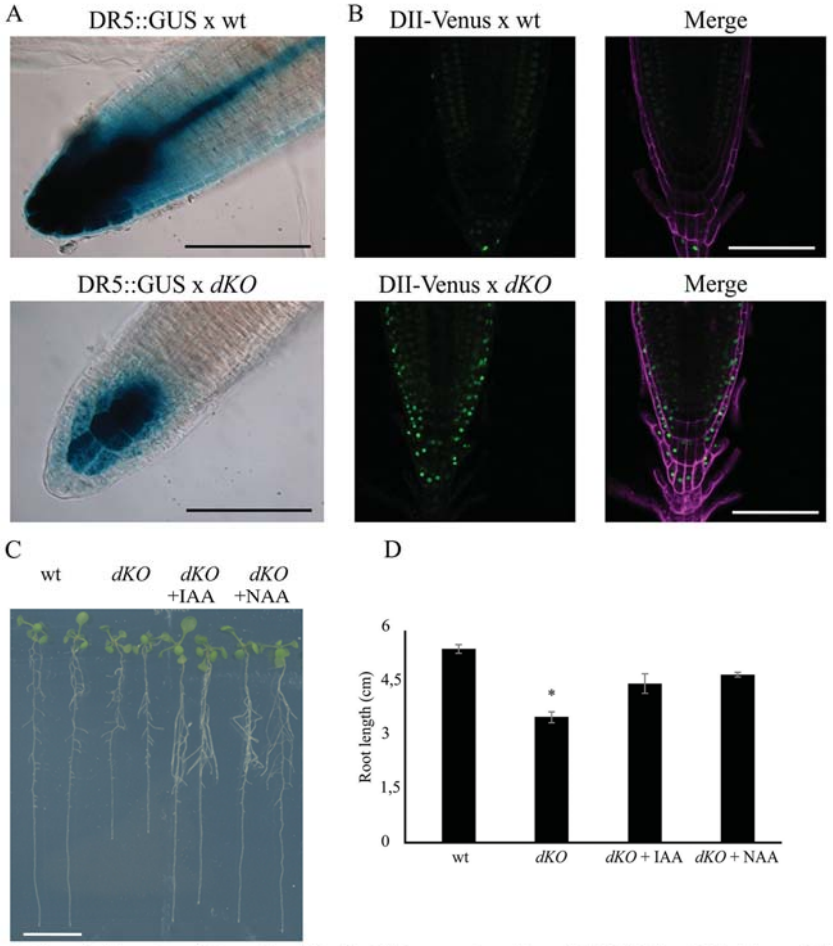

Fig. 4. Auxin distribution is altered in the root meristem of the dKO. (A) GUS expression pattern of DR5:GUS in *dKO* background (lower panel) is weaker than in DR5:GUS (upper panel). Scale bar = 100 μm. (B) The green fluorescence of DII-Venus shows much higher levels in the *dKO* background (lower panel) compared with the wild-type (upper panel), in particular in the columella cells and in the epidermis. Venus Ex: 488nm, Em: 520–540nm; PI Ex: 488nm, Em: 600–650nm. Scale bar = 100 μm. (C) *dKO* short-root phenotype is rescued by application of 10nM IAA or NAA to 5-d-old seedlings and analysed after 5 d. Scale bar = 1cm. (D) Quantification of the primary root length of wild-type and *dKO* lines under control condition or upon auxin treatment (*P<0.01, Student's t-test). (A colour version of this figure is available at *JXB* online.)

PINs expression level and localization is altered in p23 double mutants

As auxin sensing and biosynthesis are not the primary cause in determining the reduction of intracellular auxin levels in the *dKO* root, auxin transport was analysed to determine whether this process could cause the short-root phenotype of p23 mutants.

The directed cell-to-cell distribution of auxin is achieved through a system of auxin influx and efflux transporters, and auxin fluxes can be predicted based on the asymmetric plasma membrane distribution of PINs determining PAT (Bailly *et al.*, 2008). PIN transcription is enhanced through auxin and diminished by cytokinin via SHY2 (Dello Ioio *et al.*, 2008). In addition, PIN activity is finely controlled through post-translational modifications, such as phosphorylation by PID (PINOID) and D6PK (D6 PROTEIN KINASE) (Zourelidou *et al.*, 2014), which also control the polar subcellular localization of these proteins (Michniewicz *et al.*, 2007; Marhavý *et al.*, 2014).

The transcription levels of the major PAT protein were assayed, analysing the gene expression level of PIN1, PIN2, PIN3, PIN4, and PIN7 using qRT-PCR analysis. The expression of PIN1, PIN3, and PIN7 was approximately 75% in the *dKO* compared with that of the wild-type (Fig. 5A). PIN proteins undergo regulation at both transcriptional and post-transcriptional levels; thus, the translational report- ers of PIN1 and PIN7, the main acropetal auxin transport mediators, were analysed in the *dKO* background. As shown in Fig. 5B, the impaired level of expression of these two carriers is reflected by their translational reporters, as observed in 7-d-old *dKO* seedlings. Particularly, PIN1-GFP and PIN7-GFP reporters confirmed the reduced expression of these proteins in the root tip of *dKO* plants, as appreciable from

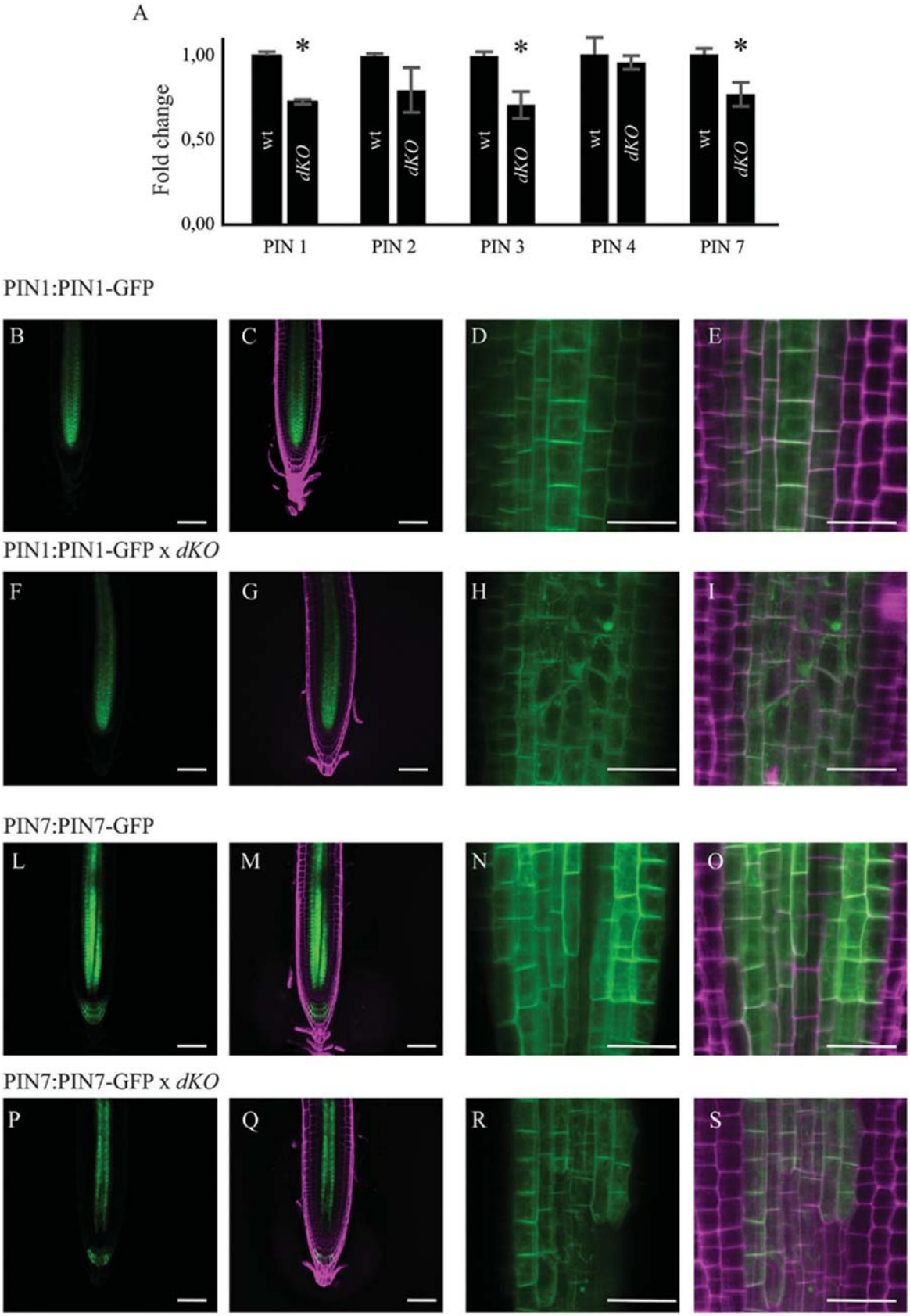

Fig. 5. PIN expression levels, and PIN1 and PIN7 localization in the *dKO*. (A) qRT-PCR of PIN1, 2, 3, 4, and 7; data were normalized to ACT2 and shown as fold change on wild-type (**P*<0.05, Student's *t*-test). (B) Confocal Laser Scanning images of PIN1 (B–E), PIN1×*dKO* (F–I) or PIN7 (L–O) and PIN7×*dKO* (P–S) showing altered expression and localization of PIN1 and PIN7 in the mutant line. GFP Ex: 488 nm, Em: 500–520 nm; PI Ex: 488 nm, Em: 600–650 nm. Scale bars (B, C, F, G, L, M, P, Q) = 50 μm; (D, E, H, I, N, O, R, S) = 10 μm. (A colour version of this figure is available at *JXB* online.)

the quantification of the GFP fluorescence in Supplementary Fig. S3 (available at *JXB* online). In addition, increased PIN1-GFP internalization into subcellular compartments of *dKO* plants was detected compared with that of the wild- type plants (Fig. 5D, E, H, I). However, alterations in the periclinal/anticlinal distribution of PIN1 and PIN7 were not observed in *dKO* mutants. Moreover, PIN7-GFP was absent in the stele cells near the stem cell niche (Fig. 5R, S). These results demonstrate that alterations in PIN expression and localization are indeed the most likely cause of lower auxin levels in p23 mutants, thus linking p23 activity to the maintenance of a correct PAT in the root meristem. In support of this hypothesis, a partial resistance of p23 mutants to treatment with NPA (Supplementary Fig. S4 available at *JXB* online), a well-known inhibitor of PAT (Bailly *et al.*, 2008), was observed. In fact, while low concentration of NPA shortened the primary root of the wild-type, a similar effect was detected in the *dKO* only with NPA concentration >1 µM.

Rescue of short-root phenotype in the triple mutant p23-1×p23-2×arr1-4

Root meristem maintenance and continuous root growth are guaranteed through a strict equilibrium between cell division and cell differentiation, which is finely controlled through plant hormone crosstalk. In this context cytokinin and auxin play key roles (Dello Ioio *et al.*, 2008; Moubayidin *et al.*, 2010; Overvoorde *et al.*, 2010; Depuydt and Hardtke, 2011; Sankar *et al.*, 2011).

For this reason, the expression of *ARR1*—a key player in cytokinin signalling—was evaluated to test the status of cytokinin signalling in the p23 double knockout mutant. As shown in Fig. 6A, *ARR1* transcripts were markedly upregulated in the *dKO* background compared with wild-type plants (7.4-fold higher). This result suggests that p23 proteins act as negative regulators of the cytokinin signalling pathway, and, at the same time, it supports a role of ARR1 in the short- root phenotype of p23 mutants. To evaluate these hypotheses, the triple mutant line *p23-1×p23-2×arr1-4* (*dKO×arr1-4*) was generated. Laser scanning confocal analysis of the PI-stained root meristem (Fig. 6B, C) showed an average meristem size of 280 µm and an average cortical cell number of 37 in the wild-type line. The p23 *dKO* mutant showed a reduced meristem length and cell number (200 µm and 25 cells, respectively), whereas the single *arr1-4* mutant showed both increased meristem length and meristematic cell number (305 µm and 41 cells), as previously described (Dello Ioio *et al.*, 2007). The triple knockout mutant *dKO×arr1-4* rescued the phenotype of the dKO, showing a meristem length and cortical cell num- ber indistinguishable from those of wild-type (280 µm and 38 cells). In addition, the *arr1-4* mutant was not completely epistatic on the *dKO*, confirming that although restoring a more equilibrated auxin/cytokinin ratio by lowering cytokinin signalling, auxin levels are not sufficient to support the meristem activity present in the single *arr1-4* mutant.

As the *dKO×arr1-4* showed a wild-type-like meristem length, the expression of PINs in this line was tested. As shown in Fig. 6D, the *arr1-4* mutant showed increased

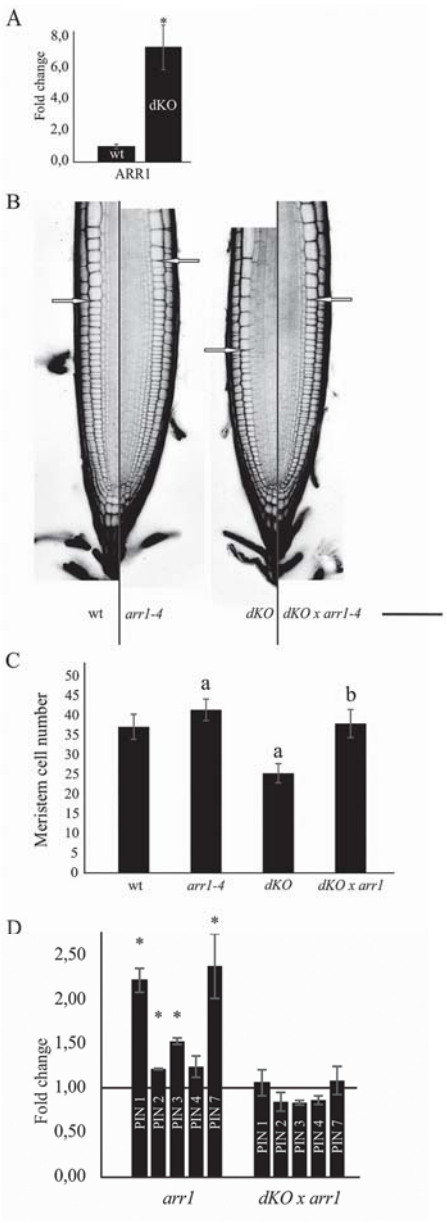

Fig. 6. Rescue of short-root phenotype in the triple mutant *p23-1×p23-2×arr1-4*. (A) qRT-PCR of *ARR1*; data were normalized to ACT2 and shown as fold change on wild-type (**P*<0.05, Student's *t*-test). (B) PI-stained root of 7-d-old seedlings of the different lines. Excitation and emission wavelength for confocal acquisition are 488nm and 600–650nm, respectively. The arrows show the upper limit of the meristematic zone. Scale bar = 50 µm. (C) Meristem cell number in the different genetic background. *dKO* mutant shows a reduced number of cortical cells in the root meristematic zone, while *arr1-4* shows an increased number of cortical cells. The triple mutant *dKO×arr1-4* shows no difference as compared with the wild-type ([a]*P*<0.01 compared with the wild-type, [b]*P*<0.01 compared with the *dKO*; both Student's *t*-test). (D) qRT-PCR of PIN1, 2, 3, 4, and 7; data were normalized to ACT2 expression and shown as fold change on wild-type (black line) (**P*<0.05, Student's *t*-test). (A colour version of this figure is available at *JXB* online.)

expression levels of PIN1, PIN2, PIN3, and PIN7, as previously described (Dello Ioio *et al.*, 2008) and the triple mutant *dKO×arr1-4* recovered PIN expression levels comparable with those of the wild-type. This result supports the prominent role of PIN expression levels in the phenotype of p23 mutants, highlighting, at the same time, an indirect role of p23 proteins on PIN expression.

Discussion

In the present study, experimental evidence on the role of the p23 co-chaperone as a novel component of the protein network regulating post-embryonic root development has been reported.

Upon seed germination, the root apical meristem grows as cell division prevails over differentiation, reaching a final size at approximately 5 dag, when a fixed meristem cell num- ber is established and meristem maintenance is guaranteed through a balance between the rate of cell differentiation and the rate of new cell generation (Blilou *et al.*, 2005; Dello Ioio *et al.*, 2007, 2008; Moubayidin *et al.*, 2009; Perilli *et al.*, 2012; Pacifici *et al.*, 2015). *Arabidopsis* p23 mutants show impaired root development due to a reduced number of cells in the root meristematic zone, where the two p23 isoforms localize. Using two specific auxin responsive markers (DR5:GUS and DII-Venus), a lower level of auxin accumulation was observed in the root tip of the mutant lines than in the wild-type. It was also shown that the short-root phenotype could be rescued both in single and double knockout mutants by supplying auxin in the growth medium (Supplementary Fig. S5 available at *JXB* online). Based on these results, a constraint at the level of auxin biosynthesis or perception can be excluded, whereas impairment in auxin distribution, reflecting alterations at the level of auxin PAT, was implied and subsequently detected. Indeed, not only were the main components of acropetal PAT—PIN1, PIN3, and PIN7—transcriptionally down-regulated but the localization patterns of PIN1-GFP and PIN7-GFP proteins were also modified. Particularly, PIN1-GFP remains, at least in part, accumulated in intra- cellular compartments and does not correctly localize to the basal membranes, whereas PIN7 showed a limited localiza- tion pattern in the root of the p23 double mutant compared with wild-type. This result suggests that altered PAT is the most likely cause of the reduced meristem length of p23 mutants. In fact, as consequence of the compromised PAT, a narrowed auxin gradient is established in the root meristem of p23 mutants, associated with a shift of the auxin maxi- mum towards the root cap (Grieneisen *et al.*, 2007), together with a reduction in its intensity.

To obtain a more complete picture of hormone signalling regulating meristem maintenance, the expression of *ARR1*—a key component of cytokinin signalling—was evaluated and an increased expression in the mutant compared with wild- type plants was observed. *ARR1*, in turn, is induced through ASB1 (Moubayidin *et al.*, 2013), whose expression wasslightly induced in the mutant. These results indicate that cytokinin signalling is enhanced in p23 mutant lines whereas the auxin signalling pathway is reduced. In addition, it was observed that a reduction in cytokinin signalling through the reduction of *ARR1* in the *dKO* mutant generates a wild-type-like phenotype. This triple mutant (*dKO×arr1-4*) shows a meristem length and a number of meristematic cortical cells similar to the wild-type, but still reduced compared with that of the *arr1-4* mutant (Dello Ioio *et al.*, 2007), thus revealing the pathway in which p23 operates. Indeed, this result provides genetic evidence that p23 primarily acts on auxin distribution in the root meristem, where these proteins are specifically expressed (Fig. 2B–G). In addition, PIN expression in the triple mutant was tested and PIN levels were found to recover to wild-type values. Taken together, these results confirm that the altered expression and localization of PIN proteins in the p23 double knockout mutant are the primary cause of the reduced meristem length and of the fewer number of meristematic cortical cells. Furthermore, the enhanced level of ARR1 expression could likely be the cause of PINs detriment in p23 mutants, and supports a role of p23 proteins in meristem maintenance a few days after germination, when ARR1 becomes the principal cytokinin effector (Pacifici *et al.*, 2015). At the same time, the recovery of PIN expression level in the triple mutant excludes a direct role of p23 proteins on PIN levels, while its role in PIN trafficking remains to be elucidated. Notably, p23 binds to HSP90 (Zhang *et al.*, 2010), which shows a specific expression at the level of the root (Krishna and Gloor, 2001). Moreover, HSP90 has been demonstrated to interact and regulate TWD1, and consequently ABCB transporters activity, a family of genes involved in extracellular auxin transport that associate with PINs (Pérez-Pérez *et al.*, 2004; Blakeslee *et al.*, 2007; Wang *et al.*, 2013). In this context, the hypothesis is presented that the absence of p23 could compromise the stability of the HSP90 complex, causing alterations in the TWD1-ABCB system, and thus on PAT, leading to reduced auxin levels in the root meristem, altered PIN expression and, as a consequence, a short-root phenotype.

Taken together, these results are consistent with increasing experimental evidence indicating that although cytokinin controls the cell differentiation rate, acting specifically at the transition zone, the graded distribution of auxin is pivotal for the dynamic regulation of root meristem size (Pacifici *et al.*, 2015). In conclusion, it is proposed that p23 sustains meristem maintenance, playing a key role in post-embryonic root growth via the regulation of auxin signalling and consequently the preservation of a balanced rate of cell differentiation and division at the transition zone.

Supplementary data

Supplementary data are available at *JXB* online.

Table S1. Primers used in genotyping, cloning, and qRT-PCR.

Figure S1. p23-1-YFP shows nuclear and cytoplasmic subcellular localization.

Figure S2. Auxin biosynthesis is not altered in the shoot of *dKO*.

Figure S3. PIN1-GFP and PIN7-GFP fluorescence quantification in the wild-type and *dKO* backgrounds.

Figure S4. *dKO* is partially insensitive to inhibition of auxin PAT.

Figure S5. Exogenous IAA rescues the short-root phenotype of p23 mutants.

Funding

This work was supported by the University of Padova [PRAT 2012, CPDA122838] and CARIPARO Foundation to SG.

Acknowledgements

We are thankful to Sabrina Sabatini for providing us with PIN1-GFP, PIN7-GFP, and *Arabidopsis* reporter lines, and for critical reading of the manuscript. We thank Alex Costa for his valuable comments and critical reading of the manuscript.

References

Ali MMU, Roe SM, Vaughan CK, Meyer P, Panaretou B, Piper PW, Prodromou C, Pearl LH. 2006. Crystal structure of an Hsp90–nucleotide–p23/Sba1 closed chaperone complex. *Nature* **440,** 1013–1017.

Bailly A, Sovero V, Vincenzetti V, Santelia D, Bartnik D, Koenig BW, Mancuso S, Martinoia E, Geisler M. 2008. Modulation of P-glycoproteins by auxin transport inhibitors is mediated by interaction with immunophilins. *Journal of Biological Chemistry* **283,** 21817–21826.

Blakeslee JJ, Bandyopadhyay A, Lee OR, *et al*. 2007. Interactions among PIN-FORMED and P-glycoprotein auxin transporters in Arabidopsis. *The Plant cell* **19,** 131–147.

Blilou I, Xu J, Wildwater M, Willemsen V, Paponov I, Friml J, Heidstra R, Aida M, Palme K, Scheres B. 2005. The PIN auxin efflux facilitator network controls growth and patterning in Arabidopsis roots. *Nature* **433,** 39–44.

Brunoud G, Wells DM, Oliva M, *et al*. 2012. A novel sensor to map auxin response and distribution at high spatio-temporal resolution. *Nature* **482,** 103–106.

Chadli A, Bouhouche I, Sullivan W, Stensgard B, McMahon N, Catelli MG, Toft DO. 2000. Dimerization and N-terminal domain proximity underlie the function of the molecular chaperone heat shock protein 90. *Proceedings of the National Academy of Sciences of the United States of America* **97,** 12524–12529.

Colón-Carmona A, You R, Haimovitch-Gal T, Doerner P. 1999. Spatio-temporal analysis of mitotic activity with a labile cyclin-GUS fusion protein. *Plant Journal* **20,** 503–508.

Depuydt S, Hardtke CS. 2011. Hormone signalling crosstalk in plant growth regulation. *Current Biology* **21,** R365–R373.

Geisler M, Murphy AS. 2006. The ABC of auxin transport: The role of p-glycoproteins in plant development. *FEBS Letters* **580,** 1094–1102.

Geisler M, Wang B, Zhu J. 2014. Auxin transport during root gravitropism: Transporters and techniques. *Plant Biology* **16,** 50–57.

Gray WM, Kepinski S, Rouse D, Leyser O, Estelle M. 2001. Auxin regulates SCF(TIR1)-dependent degradation of AUX/IAA proteins. *Nature* **414,** 271–276.

Grieneisen VA, Xu J, Marée AFM, Hogeweg P, Scheres B. 2007. Auxin transport is sufficient to generate a maximum and gradient guiding root growth. *Nature* **449,** 1008–1013.

Hellens RP, Edwards EA, Leyland NR, Bean S, Mullineaux PM. 2000. pGreen: a versatile and flexible binary Ti vector for Agrobacterium-mediated plant transformation. *Plant molecular biology* **42,** 819–832.

Dello Ioio R, Linhares FS, Scacchi E, Casamitjana-Martinez E, Heidstra R, Costantino P, Sabatini S. 2007. Cytokinins Determine Arabidopsis Root-Meristem Size by Controlling Cell Differentiation. *Current Biology* **17,** 678–682.

Dello Ioio R, Nakamura K, Moubayidin L, Perilli S, Taniguchi M, Morita MT, Aoyama T, Costantino P, Sabatini S. 2008. A genetic framework for the control of cell division and differentiation in the root meristem. *Science (New York, N.Y.)* **322,** 1380–1384.

Johnson JL, Toft DO. 1994. A novel chaperone complex for steroid receptors involving heat shock proteins, immunophilins, and p23. *The Journal of biological chemistry* **269,** 24989–24993.

Krecek P, Skupa P, Libus J, Naramoto S, Tejos R, Friml J, Zazímalová E. 2009. The PIN-FORMED (PIN) protein family of auxin transporters. *Genome biology* **10,** 249.

Krishna P, Gloor G. 2001. The Hsp90 family of proteins in Arabidopsis thaliana. *Cell stress & chaperones* **6,** 238–246.

Li J, Soroka J, Buchner J. 2012. The Hsp90 chaperone machinery: Conformational dynamics and regulation by co-chaperones. *Biochimica et Biophysica Acta - Molecular Cell Research* **1823,** 624–635.

Ljung K, Hull AK, Celenza J, Yamada M, Estelle M, Normanly J, Sandberg G. 2005. Sites and regulation of auxin biosynthesis in Arabidopsis roots. *The Plant cell* **17,** 1090–1104.

Marhavý P, Duclercq J, Weller B, Feraru E, Bielach A, Offringa R, Friml J, Schwechheimer C, Murphy A, Benková E. 2014. Cytokinin controls polarity of PIN1-dependent auxin transport during lateral root organogenesis. *Current biology : CB* **24,** 1031–1037.

Michniewicz M, Zago MK, Abas L, *et al*. 2007. Antagonistic Regulation of PIN Phosphorylation by PP2A and PINOID Directs Auxin Flux. *Cell* **130,** 1044–1056.

Mockaitis K, Estelle M. 2008. Auxin receptors and plant development: a new signaling paradigm. *Annual review of cell and developmental biology* **24,** 55–80.

Moubayidin L, Di Mambro R, Sabatini S. 2009. Cytokinin-auxin crosstalk. *Trends in Plant Science* **14,** 557–562.

Moubayidin L, Perilli S, Dello Ioio R, Di Mambro R, Costantino P, Sabatini S. 2010. The rate of cell differentiation controls the arabidopsis root meristem growth phase. *Current Biology* **20,** 1138–1143.

Moubayidin L, Di Mambro R, Sozzani R, *et al*. 2013. Spatial coordination between stem cell activity and cell differentiation in the root meristem. *Developmental cell* **26,** 405–15.

Overvoorde P, Fukaki H, Beeckman T. 2010. Auxin control of root development. *Cold Spring Harbor perspectives in biology* **2,** 1–16.

Pacifici E, Polverari L, Sabatini S. 2015. Plant hormone cross-talk : the pivot of root growth. *Journal of Experimental Botany* **66,** 1113–1121.

Pérez-Pérez JM, Ponce MR, Micol JL. 2004. The ULTRACURVATA2 gene of Arabidopsis encodes an FK506-binding protein involved in auxin and brassinosteroid signaling. *Plant physiology* **134,** 101–117.

Perilli S, Di Mambro R, Sabatini S. 2012. Growth and development of the root apical meristem. *Current Opinion in Plant Biology* **15,** 17–23.

Saini S, Sharma I, Kaur N, Pati PK. 2013. Auxin: A master regulator in plant root development. *Plant Cell Reports* **32,** 741–757.

Sankar M, Osmont KS, Rolcik J, Gujas B, Tarkowska D, Strnad M, Xenarios I, Hardtke CS. 2011. A qualitative continuous model of cellular auxin and brassinosteroid signaling and their crosstalk. *Bioinformatics* **27,** 1404–1412.

Tosoni K, Costa A, Sarno S, D'Alessandro S, Sparla F, Pinna L a., Zottini M, Ruzzene M. 2011. The p23 co-chaperone protein is a novel substrate of CK2 in Arabidopsis. *Molecular and Cellular Biochemistry* **356,** 245–254.

Ulmasov T, Murfett J, Hagen G, Guilfoyle TJ. 1997. Creation of a Highly Active Synthetic AuxRE. *Society* **9,** 1963–1971.

Verrier PJ, Bird D, Burla B, *et al*. 2008. Plant ABC proteins--a unified nomenclature and updated inventory. *Trends in plant science* **13,** 151–159.

Vieten A, Sauer M, Brewer PB, Friml J. 2007. Molecular and cellular aspects of auxin-transport-mediated development. *Trends in plant science* **12,** 160–168.

Wang B, Bailly A, Zwiewka M, Henrichs S, Azzarello E, Mancuso S, Maeshima M, Friml J, Schulz A, Geisler M. 2013. Arabidopsis TWISTED DWARF1 functionally interacts with auxin exporter ABCB1 on the root plasma membrane. *Plant Cell* **25,** 202–214.

Zhang Z, Sullivan W, Felts SJ, Prasad BD, Toft DO, Krishna P. 2010. Characterization of plant p23-like proteins for their co-chaperone activities. *Cell Stress and Chaperones* **15,** 703–715.

Zourelidou M, Absmanner B, Weller B, *et al*. 2014. Auxin efflux by PIN-FORMED proteins is activated by two different protein kinases, D6 PROTEIN KINASE and PINOID. *eLife* **3,** e02860.

REFERENCES

Borisjuk L, Walenta S, Rolletschek H, Mueller-Klieser W, Wobus U, Weber H. (2002) Spatial analysis of plant metabolism: sucrose imaging within Vicia faba cotyledons reveals specific developmental patterns. *Plant J.* 29(4):521-30.

Boyes DC, Zayed AM, Ascenzi R, McCaskill AJ, Hoffman NE, Davis KR, Görlach J. (2001) Growth stage-based phenotypic analysis of Arabidopsis: a model for high throughput functional genomics in plants. *Plant Cell.* 13(7):1499-510.

Cai Q, Guo L, Shen ZR, Wang DY, Zhang Q, Sodmergen. (2015) Elevation of Pollen Mitochondrial DNA Copy Number by WHIRLY2: Altered Respiration and Pollen Tube Growth in Arabidopsis. *Plant Physiol.* 169(1):660-73.

Cappadocia L, Maréchal A, Parent JS, Lepage E, Sygusch J, Brisson N. (2010) Crystal structures of DNA-Whirly complexes and their role in Arabidopsis organelle genome repair. *Plant Cell.* 22(6):1849-67.

Carrie C, Whelan J. (2013) Widespread dual targeting of proteins in land plants: when, where, how and why. Plant Signal Behav. 8(8).

Cupp JD, Nielsen BL. (2013) Arabidopsis thaliana organellar DNA polymerase IB mutants exhibit reduced mtDNA levels with a decrease in mitochondrial area density. *Physiol Plant.* 149(1):91-103.

De Clercq I, Vermeirssen V, Van Aken O, Vandepoele K, Murcha MW, Law SR, Inzé A, Ng S, Ivanova A, Rombaut D, van de Cotte B, Jaspers P, Van de Peer Y, Kangasjärvi J, Whelan J, Van Breusegem F. (2013) The membrane-bound NAC transcription factor ANAC013 functions in mitochondrial retrograde regulation of the oxidative stress response in Arabidopsis. *Plant Cell.* 25(9):3472-90.

de Souza A, Wang JZ, Dehesh K. (2017) Retrograde Signals: Integrators of Interorganellar Communication and Orchestrators of Plant Development. *Annu Rev Plant Biol.* 28;68:85-108.

Desveaux D, Subramaniam R, Després C, Mess JN, Lévesque C, Fobert PR, Dangl JL, Brisson N. (2004) A "Whirly" transcription factor is required for salicylic acid-dependent disease resistance in Arabidopsis. *Dev Cell.* 6(2):229-40.

Desveaux D, Allard J, Brisson N, Sygusch J. (2002) A new family of plant transcription factors displays a novel ssDNA-binding surface. *Nat Struct Biol.* 9(7):512-7.

Doughty J, Aljabri M, Scott RJ. (2014) Flavonoids and the regulation of seed size in Arabidopsis. *Biochem Soc Trans.* 42(2):364-9.

Kalve S, De Vos D, Beemster GTS. (2014) Leaf development: a cellular perspective. Frontiers in *Plant Science* 5, 362.

Krause K, Kilbienski I, Mulisch M, Rödiger A, Schäfer A, Krupinska K. (2005) DNA-binding proteins of the Whirly family in Arabidopsis thaliana are targeted to the organelles. *FEBS Lett.* 579(17):3707-12.

Kumar RA, Bendich AJ. (2011) Distinguishing authentic mitochondrial and plastid DNAs from similar DNA sequences in the nucleus using the polymerase chain reaction. *Curr Genet.* 57(4):287-95.

Krupinska K, Oetke S, Desel C, Mulisch M, Schäfer A, Hollmann J, Kumlehn J, Hensel G. (2014) WHIRLY1 is a major organizer of chloroplast nucleoids. *Front Plant Sci.* 4;5:432.

Estavillo GM, Chan KX, Phua SY, Pogson BJ. (2013) Reconsidering the nature and mode of action of metabolite retrograde signals from the chloroplast. *Front Plant Sci.* 4;3:300.

Foyer CH, Karpinska B, Krupinska K. (2014) The functions of WHIRLY1 and REDOX-RESPONSIVE TRANSCRIPTION FACTOR 1 in cross tolerance responses in plants: a hypothesis. *Philos Trans R Soc Lond B Biol Sci.* 369(1640):20130226.

Frey TG, Mannella CA (2000) The internal structure of mitochondria. *Trends Biochem Sci.* 25(7):319-24.

Gaff D.F. and Okong'O-Ogola O (1971) The Use of Non-permeating Pigments for Testing the Survival of Cells. *Journal of Experimental Botany* 22, 756–758.

Grabowski E, Miao Y, Mulisch M, Krupinska K. (2008) Single-stranded DNA-binding protein Whirly1 in barley leaves is located in plastids and the nucleus of the same cell. *Plant Physiol.* 147(4):1800-4.

Giraud E, Van Aken O, Ho LH, Whelan J. (2009) The transcription factor ABI4 is a regulator of mitochondrial retrograde expression of ALTERNATIVE OXIDASE1a. *Plant Physiol.* 150(3):1286-96.

Gray JC, Hansen MR, Shaw DJ, Graham K, Dale R, Smallman P, Natesan SK, Newell CA. (2012) Plastid stromules are induced by stress treatments acting through abscisic acid. *Plant J.* 69(3):387-98.

Han C and Yang P. (2015) Studies on the molecular mechanisms of seed germination. *Proteomics.* 15(10):1671-9.

Horbay R, Bilyy R. (2016) Mitochondrial dynamics during cell cycling. *Apoptosis.* 21(12):1327-1335.

Howell KA, Millar AH, Whelan J. (2006) Ordered assembly of mitochondria during rice germination begins with pro-mitochondrial structures rich in components of the protein import apparatus. *Plant Mol Biol.* 60(2):201-23.

Isemer R, Mulisch M, Schäfer A, Kirchner S, Koop HU, Krupinska K. (2012) Recombinant Whirly1 translocates from transplastomic chloroplasts to the nucleus. *FEBS Lett.* 586(1):85-8.

Juszczuk IM, Szal B, Rychter AM. (2012) Oxidation-reduction and reactive oxygen species homeostasis in mutant plants with respiratory chain complex I dysfunction. *Plant Cell Environ.* 35(2):296-307.

Lastdrager J, Hanson J, Smeekens S. (2014) Sugar signals and the control of plant growth and development. *J Exp Bot.* 65(3):799-807.

Lee SR, Han J (2017). Mitochondrial Nucleoid: Shield and Switch of the Mitochondrial Genome. *Oxid Med Cell Longev.* 2017:8060949

Leister D. (2012) Retrograde signaling in plants: from simple to complex scenarios. *Front Plant Sci.* 19;3:135.

Logan DC. (2006) The mitochondrial compartment. *J Exp Bot.* 57(6):1225-43.

Maréchal A, Parent JS, Véronneau-Lafortune F, Joyeux A, Lang BF, Brisson N. (2009) Whirly proteins maintain plastid genome stability in Arabidopsis. *Proc Natl Acad Sci U S A.* 106(34):14693-8.

Maréchal A, Parent JS, Sabar M, Véronneau-Lafortune F, Abou-Rached C, Brisson N (2008) Overexpression of mtDNA-associated AtWhy2 compromises mitochondrial function. *BMC Plant Biol.* 18, 8-42

Melonek J, Mulisch M, Schmitz-Linneweber C, Grabowski E, Hensel G, Krupinska K. (2010) Whirly1 in chloroplasts associates with intron containing RNAs and rarely co-localizes with nucleoids. *Planta.* 232(2):471-81.

Meng LS, Xu MK, Li D, Zhou MM, Jiang JH. (2017) Soluble Sugar Accumulation Can Influence Seed Size via AN3-YDA Gene Cascade. *J Agric Food Chem.* 24;65(20):4121-4132.

Murashige T, Skoog F. (1962) A revised medium for rapid growth and bioassays with tobacco tissue cultures. *Physiol Plantarum* 15: 473–497.

Murcha MW, Wang Y, Narsai R, Whelan J. (2014) The plant mitochondrial protein import apparatus - the differences make it interesting. *Biochim Biophys Acta.* 1840(4):1233-45.

Li N, Li Y. (2016) Signaling pathways of seed size control in plants. *Curr Opin Plant Biol.* 33:23-32.

Livak K.J. and Schmittgen T.D. (2001) Analysis of relative gene expression data using real-time quantitative PCR and the 2(-Delta Delta C(T)). *Methods* 25, 402-408.

Ng S, Ivanova A, Duncan O, Law SR, Van Aken O, De Clercq I, Wang Y, Carrie C, Xu L, Kmiec B, Walker H, Van Breusegem F, Whelan J, Giraud E. (2013) A membrane-bound NAC transcription factor, ANAC017, mediates mitochondrial retrograde signaling in Arabidopsis. *Plant Cell.* 25(9):3450-71.

Osuna D, Prieto P, Aguilar M. (2015) Control of Seed Germination and Plant Development by Carbon and Nitrogen Availability. *Front Plant Sci.* 18;6:1023.

Parent JS, Lepage E, Brisson N. (2011) Divergent roles for the two PolI-like organelle DNA polymerases of Arabidopsis. *Plant Physiol.* 156(1):254-62.

Pfannschmidt T. (2010) Plastidial retrograde signalling--a true "plastid factor" or just metabolite signatures? *Trends Plant Sci.* 15(8):427-35.

Preuten T, Cincu E, Fuchs J, Zoschke R, Liere K, Börner T. (2010) Fewer genes than organelles: extremely low and variable gene copy numbers in mitochondria of somatic plant cells. *Plant J.* 64(6):948-59.

Raghavendra AS, Padmasree K. (2003) Beneficial interactions of mitochondrial metabolism with photosynthetic carbon assimilation. *Trends Plant Sci.* 8(11):546-53.

Saha B, Borovskii G, Panda SK. (2016) Alternative oxidase and plant stress tolerance. *Plant Signal Behav.* 11(12).

Sano N, Rajjou L, North HM, Debeaujon I, Marion-Poll A, Seo M. (2016) Staying Alive: Molecular Aspects of Seed Longevity. *Plant Cell Physiol.* 57(4):660-74.

Sato T, Maekawa S, Yasuda S, Sonoda Y, Katoh E, Ichikawa T, Nakazawa M, Seki M, Shinozaki K, Matsui M, Goto DB, Ikeda A, Yamaguchi J. (2009) CNI1/ATL31, a RING-type ubiquitin ligase that functions in the carbon/nitrogen response for growth phase transition in Arabidopsis seedlings. *Plant J.* 60(5):852-64.

Scialdone A, Howard M. (2015) How plants manage food reserves at night: quantitative models and open questions. *Front Plant Sci.* 31;6:204.

Sun X, Feng P, Xu X, Guo H, Ma J, Chi W, Lin R, Lu C, Zhang L. (2011) A chloroplast envelope-bound PHD transcription factor mediates chloroplast signals to the nucleus. *Nat Commun.* 20;2:477.

Susek RE, Ausubel FM, Chory J. (1993) Signal transduction mutants of Arabidopsis uncouple nuclear CAB and RBCS gene expression from chloroplast development. *Cell.* 10;74(5):787-99.

Weitbrecht K, Müller K, Leubner-Metzger G. (2011) First off the mark: early seed germination. *J Exp Bot.* 62(10):3289-309.

Winter D, Vinegar B, Nahal H, Ammar R, Wilson GV, Provart NJ. (2007) An "Electronic Fluorescent Pictograph" browser for exploring and analyzing large-scale biological data sets. *PLoS One.* 8;2(8)

Woodson JD, Chory J. (2008) Coordination of gene expression between organellar and nuclear genomes. *Nat Rev Genet.* 9(5):383-95.

Van Dingenen J, Blomme J, Gonzalez N, Inzé D (2016) Plants grow with a little help from their organelle friends. *J Exp Bot.* 67(22):6267-6281.

Vanlerberghe GC. (2013) Alternative oxidase: a mitochondrial respiratory pathway to maintain metabolic and signaling homeostasis during abiotic and biotic stress in plants. *Int J Mol Sci.* 14(4):6805-47.

Verma, P., Kaur, H., Petla, B. P., Rao, V., Saxena, S. C. and Majee, M. (2013). PROTEIN L-ISOASPARTYL METHYLTRANSFERASE2 is differentially expressed in chickpea and enhances seed vigor and longevity by reducing abnormal isoaspartyl accumulation predominantly in seed nuclear proteins. *Plant Physiol* 161(3): 1141-1157.